공학박사학위논문

압전재료 입자와 형상기억합금 입자를 사용한 탄소섬유 강화복합재료의 진동감쇠향상

Passive vibration damping of CFRP with PZT and SMA particles

서울대학교 대학원
기계항공공학부
정 재 민

Passive vibration damping of CFRP with PZT and SMA particles

Jaemin Jung
School of Mechanical and Aerospace Engineering
Seoul National University

Abstract

Carbon fiber reinforced plastic (CFRP) has been widely used for various industrial areas such as aerospace, automotive, civil engineering and leisure and sports goods industries because of its high strength-to-weight ratio, low density, good thermal properties and other great mechanical properties. However, in spite of these advantages, it is not suitable for some structures that have to endure much vibration due to its low damping capacity. Therefore, some researchers have been conducted about improving a damping capability of CFRP composites recently.

In this research, the piezoelectric ceramic particles used as a functional particle which accelerates the loss of the vibration energy. Shape memory alloy (SMA) is commonly known as a kind of hyperelastic materials, which can improve the damping capacity of the CFRP. When the shape of the materials is

changed, its phase and crystal structure are changed, therefore, the mechanical energy is converted into the thermal energy as a result.

This study covers CFRP composites, which have a high damping capacity with lead zirconate titanate (PZT) ceramic particles and SMA powder dispersed between carbon fiber and epoxy matrix. The loss factor (tanδ) is measured using dynamic mechanical analyzer (DMA) to verify the structure change in vibration damping.

Experimental results show that the vibration damping of CFRP containing PZT and SMA is higher than that of conventional materials. We also found that the dispersion of particles inside the CFRP is an important factor in improving vibration damping.

In order to improve the dispersion of PZT and SMA particles in CFRP, we fabricated a thin resin film with dispersed particles. Because of applying this to CFRP, it is confirmed that the increase of dispersion degree positively affects vibration damping improvement. The 0-3 composites were modeled containing PZT and SMA particles and performed computational analysis on various parameters to verify the experimental results and optimize the parameters.

Keywords: Vibration damping, Carbon fiber reinforced plastic (CFRP), Piezoelectric

effect, Lead zirconate titanate (PZT), Shape memory alloy (SMA), Dynamic mechanical analyzer (DMA), Loss factor (tanδ).

Contents

List of figures

List of tables

Chapter 1. Introduction

1.1. Overview

Composite materials have been used for a long time in history, by mixing several materials to complement the properties of the material and to show better properties. Composite materials have been widely used in the history of humankind, such as bricks with straw, reinforced concrete, and composite bow. However, in the current composite market, composite materials are dominated by fiber-reinforced composites. Glass fiber reinforced plastics, which began to be used in the early 1940s, are the beginning. The fiber-reinforced composites are materials that can achieve high strength with lightweight and consist of fibers that are reinforcing materials and polymer matrix materials [1-5]. The reinforcing fibers support the load, and the matrix acts to hold the fibers in the desired direction and to transfer the load between the fibers. Especially, it is used in various fields because it can obtain desired physical properties according to selection of reinforcing fiber and matrix material. Carbon fiber reinforced plastic (CFRP) is used in a wide range of applications due to its strength, heat resistance and corrosion resistance, despite its light weight

compared with other materials [1-9]. In aerospace, the trend is to increase the proportion of composites in parts for aircraft weight reduction and corrosion resistance. Especially in the leisure / sports industry, it is widely used in the production of golf shafts, tennis racquets, ski and snowboards due to the above advantages. In recent years, nano/micro materials have been used as reinforcing materials in place of reinforcing fibers, and nano/micro materials have been added to polymer materials as matrix materials to make base materials having better mechanical properties and to use them in composite materials. However, in spite of these advantages, it is not suitable for some structures, which have to endure much vibration due to its low damping capacity [1-9]. Therefore, recently, various studies have been conducted to improve the vibration damping ability of CFRP, and studies on functional composite materials, which can absorb the shock, are in progress. In this study, we made CFRP composites, which have a high damping capacity with lead zirconate titanate (PZT) ceramic particles and SMA powder dispersed between carbon fiber and epoxy matrix. The loss factor (tanδ) is measured using dynamic mechanical analyzer (DMA) to verify the structure change in vibration damping.

1.2. Literature survey

1.2.1. Damping of composite material

For enhancing the damping capacity of CFRP composites, active and passive damping system can be applied. In the active damping, a sensor that takes a vibration signal from the outside is attached to the system and it makes some opposite signal to reduce the vibration [2]. Active damping system is a quite precise way to control the vibration, but it is more complicate to design the whole structure. On the other hand, passive damping system is to put some materials, which can reduce the vibration itself between carbon fiber and matrix of the composites. Although it is less effective way to improve a damping ability than the active system, the passive system is easy to apply to the structures. There are several ways to enhance passive vibration damping of composite. First, viscoelastic materials are one of the materials, which can enhance the damping capacity by thermos-viscoelastic heat generation [3]. However, viscoelastic materials may decrease the mechanical properties of the whole structure. Second, micro/nanoparticles like carbon nanotube (CNT) and carbon black can be dispersed in the composites and they could increase

damping capacity by converting the vibration energy into the frictional heat [4]. Third, multifunctional materials, which contain the piezoelectric material, shape memory, alloy (SMA). These materials, so called “Active materials”, can convert a non-mechanical input into a mechanical output, or vice versa. The mechanical response of these materials to the non-mechanical input is several orders of magnitude greater than thermal expansion. Piezoelectric material converts the mechanical energy into the electrical and the electrical energy into mechanical energy [5-9]. Shape memory alloy (SMA) is also commonly known as a kind of hyperelastic materials, which can could be restore their shape when reaching particular temperature. When the shape of the materials is deformed, its phase and crystal structure are changed. Therefore, the mechanical energy is converted into the thermal energy as a result. Uchino and Ishii [6] increased the ability of the vibration damping of composite materials with piezoelectric ceramic particles. In this research, the piezoelectric ceramic particles used as a functional particle, which accelerates the loss of the vibration energy, improve the damping capacity of the CFRP. Using this phenomenon, there are some researches about the vibration damping systems with SMA particles [7].

1.2.2. Piezoelectric material

Pierre and Jacque Curie discover the piezoelectric effect in 1880 after the phenomenon of voltage generation when the deformation was applied to the crystals of crystals. PZT is a typical piezoelectric ceramics material used in various fields such as microphones, speakers, and actuators. Electrical energy is generated by deformation of the piezoelectric ceramic particles during vibration of the composite material, which can lead to current flow if proper resistance is present [5-9]. Since the joule heat consumes the generated current as it passes through the resistor, it can be seen that the vibration energy is converted into thermal energy, which increases the vibration damping ability of the material. According to Tanimoto [9], the carbon fiber-reinforced composite material can function as a proper resistor, so that the vibration damping mechanism of the piezoelectric ceramics can be applied. He applied the trial and error method to find the optimum content of piezoelectric ceramic particles. The vibration damping capability of composites by piezoelectric ceramic particles increases as the electrical connections of the piezoelectric ceramic particles and the carbon fibers, which serve as resistors. To obtain the ideal vibration damping capability through particles, the piezoelectric ceramic particles should be

distributed in a close-packed plane structure of one layer of the composite material.

The content of particles per unit area that can be expected in such a structure is calculated as follows.

The ∅ is the mean diameter of the particles and ρ is the density of the particles. Based on these equations, it would be possible to calculate the optimum particles content per area [5]. These electrical properties can also be used to monitor the life of composite materials. Schueler et al. [10] proposed that carbon fiber-reinforced composites themselves could be considered as self-monitoring materials because carbon fiber itself can be considered as a good conductive material. The mechanical properties of the carbon fiber reinforced composite material depend on the properties of the carbon fiber so that the fracture of the carbon fiber results in deterioration of the overall mechanical properties of the composite material. However, if an electrical signal is passed through the carbon fiber in the composite material and the resistance or electrical conductivity thereof can be measured, the damage of the carbon fiber can be monitored.

1.2.3. Shape memory alloy

Shape memory alloys (SMA) are a type of shape memory material that can recover shape when temperature increases. As the temperature increases, it can lead to shape recovery even under high applied loads, resulting in high operating energy density. In addition, under certain conditions, SMA can absorb or dissipate mechanical energy by experiencing reversible hysteresis shape changes when applied to mechanical cyclic loads. Due to the inherent characteristics of these SMA, it is widely used in sensor and actuator, shock absorption and vibration damping applications [11]. However, SMA shows low frequency response as shown in Figure 2. A higher operating frequency can be achieved in a class of SMA, called the recently studied magnetic shape memory alloys. The application of SMA spans a variety of industries, including aerospace, automotive, biomedical and oil exploration. In the last decades, there have been several important studies exploring the microstructure mechanism, engineering effects and applications of shape memory alloys, including the application of Jackson's joint research [12], Duerig and other studies [13].

In addition, the addition of SMA powder or fiber to the composite improves the vibration damping ability of the composite material as well as the

deformation caused by the phase change. When the austenite (the steel and the alloy steel forming the face centered cubic structure in which the alloy element is melted) is cooled, it becomes a twin martensite phase that is a low temperature phase. When the material is deformed in this low temperature state and then heated, it returns to its original shape. One-way memory is used to memorize only one shape of a high-temperature image, and if the shape is repeated many times between high and low temperatures, both high and low temperatures can be memorized. It is called two-way memory. Generally, the unidirectional shape recovery force is generated by heating, and when it is cooled again, if it is recovered to a low temperature shape, it will have a biodegradable shape recovery force.

1.3. Scope of this study

In this study, the particles of lead zirconate titanate (PZT) ceramics, which is one of the typical piezoelectric materials, are applied to the CFRP fabrication process, so that carbon fiber inside the composite material is used as a resistor and electricity generated from the deformation of PZT is used as a power source. A simple electrical circuit is used to convert the vibration energy into

electrical energy and thermal energy to increase the vibration damping ability. In addition, we understand the mechanism that causes this effect, and by doing this, we want to make an optimal way to increase vibration damping ability of CFRP. Shape memory alloy (SMA) is also commonly known as a kind of hyperelastic materials, which can improve the damping capacity of the CFRP. When the shape of the materials is changed, its phase and crystal structure are changed, therefore, the mechanical energy is converted into the thermal energy as a result. Using this phenomena, there are some researches about the vibration damping systems with SMA particles. According to the materials study, SMA and PZT have different actuation frequency ranges [11]. As shown in Figure 2, actuation frequency range of SMA is differ from PZT actuation range. It is expected that the range of frequencies at which the vibration damping effect is maximized will be different when PZT and SMA particles are applied to the carbon fiber reinforced composite material. The loss factor is used as a parameter to indicate the vibration damping capability, which is measured using a dynamic mechanical analyzer (DMA). Through the above-mentioned method, the effective dispersion method for effectively applying the PZT ceramic particles and SMA particles to the inside of the CFRP is studied. Moreover, the modeling of vibration damping mechanism through the PZT ceramic particles

and SMA particles is conducted and analyzed. Moreover, the finding of application field is the goal of this study.

Chapter 2. DMA analysis of CFRP with PZT and SMA particles

2.1. Overview

In this chapter, specimens were fabricated to confirm the vibration damping effect of carbon fiber reinforced composites containing PZT and SMA particles. Specimens were prepared with different particle contents and control specimens with particles, which have no functional effect, were prepared. The analysis was carried out through two test methods. First, a 3-point bending test was conducted using a universal testing machine (UTM) to measure the bending stiffness. Second, using dynamic mechanical analyzer (DMA), the vibration damping of composite is measured. The sizes and shapes of the specimens were the same as those of the DMA specimens prepared above. The test carried out using 25 specimens per each particles loading. The vibration damping capacity change of the material measured to 3-point bending mode in frequency sweep using dynamic mechanical analyzer. The measured value is the loss factor (tanδ) of the material, of which the parameter is representing the vibration damping of the material. The loss factor (tanδ) is measured by DMA (Dynamic mechanical

analyzer) which is used to measure the viscoelastic behavior of a material to verify the change in vibration damping. For each material content, the data were obtained and the average value of 25 specimens was used as a result. In addition, we conducted the same experiment using titanium dioxide (TiO_2) particles, which do not have the piezoelectric effect to compare the vibration damping ability increase by friction and by electrical heat caused by PZT. The results show that there exists difference on vibration damping ability between CFRP with PZT ceramic particles and CFRP with TiO_2 particles.

2.2. Materials

The PZT particles (average diameter: ~10um) are made of pre-poled PZT film, PIC-151 from PI ceramic. Its density is 7.8g/cm3, piezoelectric coefficient d33 is 500 pC/N, and Curie temperature is 250˚C. PZT particles are milled by ball milling machine. Further, it sieved by 20um metal sieve. Nickel titanium is most commonly used shape memory alloy. NiTi powder is sieved by 20um metal sieve. Its average particle diameter is about 10 um. Figure 1 shows SEM images of PZT particles and SMA powder. Unidirectional carbon prepreg is USN-150B from SK Chemical (Korea). Carbon fiber reinforced plastic composites with TiO_2 particles were made of same prepreg above and TiO_2

particles with (Alfa Aesar, US) 1-2um in diameter. The carbon black was Raven 7000 from Sehan Silichem and the average diameter was 11 nm.

2.3. Specimen preparation

Carbon fiber reinforced plastic composites were made of unidirectional carbon fiber prepreg by using hand layup and hot press method. Four sheets of prepreg were laminated with unidirectional (0° direction), and the PZT ceramic particles were dispersed in every interlayer. The amount of dispersed PZT particles varied from $0\,g/m^2$ to $35\,g/m^2$ in increments of $5\,g/m^2$. Therefore, eight types of specimens were manufactured with 5 specimens in each type. Laminated prepreg was cured for 2hours, at the temperature of 130°C, and the pressure of 2.2bar using a hot-press. Specimens were produced according to the ASTM 5023 standard with 65mm in length, 13mm in width, and 0.6mm in thickness [8]. CFRP specimens with SMA particles were made by following the same manufacturing process of composite materials with PZT particles. The loading of SMA particles varied from $0\,g/m^2$ to $35\,g/m^2$ in increments of $5\,g/m^2$. Eight types of specimens were manufactured with 5 specimens in each type. CFRP specimens with TiO_2 particles were made by following the same

manufacturing process of composite materials with PZT particles. The loading of TiO_2 particles varied from $0\ g/m^2$ to $20\ g/m^2$ in increments of $5\ g/m^2$. Five types of specimens were manufactured with five specimens in each type.

2.4. Results

2.4.1. Flexural modulus test

As the result of the measurement of the bending stiffness of the material, the stiffness of the composite material including the mixture of PZT and PZT with carbon black was not significantly different from that of the specimen without any stiffness. The measured values showed no significant change from the mean value. This indicates that the added material does not act as a drawback that greatly degrades the mechanical properties of the material. The purpose of this study is to maintain the mechanical properties of the material and increase the vibration damping of the material. Therefore, it is considered that the inclusion of the particles does not significantly affect the bending stiffness. However, the surface bond strength between the inserted particles and the polymer matrix is expected to be weaker than the strength between the fibers and the matrix. Therefore, particles are expected to weaken inter laminar properties and Mode 1

fracture toughness of the composite.

2.4.2. DMA results of CFRP with PZT particles at 120Hz

The DMA test results of the carbon fiber composite specimen containing only PZT show that the loss factor changes depending on the content. As the result of the test at 120Hz, the vibration damping of the composite increases with the content of PZT particles in the composite, but it does not increase any more after $15\mathrm{g}/m^2$. PZT particles are ceramic particles and do not have electrical conductivity. Therefore, when a large amount of particles is dispersed, the effective contact area with the electrically conductive carbon fiber is decreased and the vibration damping effect is reduced.

2.4.3. DMA results of CFRP with TiO_2 particles at 120Hz

In case of CFRP with TiO_2 particles, the frequency-dependent DMA test results of the carbon fiber composite specimen confirmed that the vibration damping ability increases about up to 13 percent than that of reference sample. However, as the loading of TiO_2 particles increases, there is no tendency for the loss factor to increase significantly. Compared to the CFRP with PZT particles specimen, the PZT specimen has a much higher loss factor value at $15\mathrm{g}/m^2$.

Since the TiO_2 specimen does not have a piezoelectric effect, the vibration damping effect is due to dissipation by frictional heat between the matrix and the particles. As a result, we have indirectly confirmed the heat loss mechanism of the vibration energy by the formation of the electrical circuit of PZT.

2.4.4. DMA results of CFRP with PZT particles, frequency sweep mode

The loss factor of carbon fiber reinforced plastic with PZT particles has maximum value at 120Hz and it can be seen that loss factor of PZT loading of $15\mathrm{g}/m^2$specimen is higher than any other specimens are. The loss factor of PZT loading of $15\mathrm{g}/m^2$ specimen at 120Hz increase 70% compare to base specimen. The vibration damping of specimens that has more PZT loading than $15\mathrm{g}/m^2$ decrease, instead. From this result, it can be considered that vibration damping enhancement of carbon fiber reinforced plastic with PZT particles has optimum value depending on PZT loading. These results imply that electrical interaction between PZT and carbon fiber causes vibration damping of carbon fiber reinforced plastic with PZT particles. Because PZT is nonconductor in itself, the more PZT loading increase over $15\,\mathrm{g}/m^2$, the less electrical connection build between PZT and carbon fiber.

2.4.5. DMA results of CFRP with SMA particles, frequency sweep mode

Figure13 and figure 14 show frequency and loss factor changes with SMA loading. As the loading of SMA powder increases, the loss factor is steadily increasing, unlike carbon fiber reinforced plastics with PZT particles. The loss factor of the carbon fiber-reinforced plastic with the SMA load of $30\mathrm{g}/m^2$specimen has the maximum value at 100 Hz. At 100 Hz, the SMA loading loss factor of the $30\mathrm{g}/m^2$ specimen is increased about 35% compared to the base specimen. However, the loss factor value of SMA $35\mathrm{g}/m^2$ loading specimen is lower than the loss factor value of SMA $30\mathrm{g}/m^2$ loading specimen. SMA has manual vibration attenuation characteristics. Therefore, the higher the SMA content, the better the vibration damping. Nevertheless, the excessive increase of SMA reduces the vibration damping due to the decrease of the resin content.

As shown in figure 15, compare CFRP with PZT to CFRP with SMA, there is slight difference of the optimum loading condition in which the vibration damping ability of the each samples are maximized. The optimum frequency of PZT is higher than frequency of SMA by 20Hz. The maximum increase in loss factor of PZT is about 70% at 120Hz.

The maximum increase of loss factor of SMA is about 35% at 100Hz. The increment of PZT specimen loss factor is larger than that of SMA's.

2.5. Summary

In this chapter, in order to improve the vibration damping ability of carbon fiber-reinforced composite materials, PZT ceramic particles dispersed carbon fiber reinforced composites were fabricated. Furthermore, to confirm the contribution of piezoelectric effect on vibration damping increase, by using the TiO_2 particles that do not have piezoelectric effect, we performed the same experiment by creating specimens in the same manner. As the experimental results, the addition of PZT ceramic particles improves the vibration damping performance of the carbon fiber reinforced composite material. Until a certain amount of loading of PZT ceramic particles, increasing PZT loading also increases the vibration damping ability. However, more than a certain amount of PZT loading disturbs to increase the vibration damping ability, rather makes decrease. The experimental results of CFRP with TiO_2 particles showed a different tendency from the result of PZT. There exists optimum value of loading in PZT experiment. However, the experimental results of CFRP with

TiO_2 particles have no optimum value of loading. Therefore, it means that the two substances act as different mechanisms in increasing the vibration attenuation ability.

I made carbon fiber reinforced plastic (CFRP) composites with lead zirconate titanate (PZT) particles and shape memory alloy (SMA) in order to improve the vibration damping ability of the CFRP. The loss factor (tanδ) is measured using dynamic mechanical analyzer (DMA) to verify viscoelastic behavior of a material. Although both materials have the effect to increase vibration damping ability of CFRP, the mechanism of energy dissipation of each material is different. Therefore, they have difference in optimum loading and vibration frequency. Based on the result, we expect that carbon fiber reinforced plastic composites, which contain PZT, and SMA simultaneously has better vibration damping capacity.

Chapter 3. Composite passive damping using particles dispersed resin film

3.1. Overview

As mentioned in chapter 1, the method to improve the vibration damping ability ideally when CFRP is made by adding PZT ceramic particles is to manufacture PZT ceramic particles by dispersing the ceramic particles on the prepreg in a single layer. In addition, PZT ceramic particles in the PZT-CFRP manufacturing process are distributed on the interlayer, so if they are not dispersed well, they may cause defects. Therefore, the dispersion of PZT ceramic particles is a very important parameter in the manufacturing process. In order to increase the degree of particles dispersion, PZT ceramic particles were dispersed in resin to make PZT resin film.

As can be seen from the results of Chapter 2, the vibration damping can be increased by adding PZT and SMA inside the carbon fiber reinforced composite. . However, in chapter 1 and chapter 2, it is confirmed that the PZT and SMA had different frequency range to maximize the vibration damping effect is different.

As shown in Fig. 18, when the SMA and PZT are applied at the same time, the influence of the two substances is reinforced, and it is expected that a passive vibration attenuating material capable of improving vibration damping in a wide range of frequencies can be produced. Therefore, in this chapter, a study was conducted to optimize the effect of the functional particles identified above. First, we have established a process for fabricating thin resin films containing particles to increase the dispersion within the composites of PZT and SMA particles. By dispersing the particles evenly inside the resin film and applying them to the carbon fiber reinforced composite material. The vibration damping ability of the composite material will increase. Second, a resin film containing particles of various conditions was applied to a composite material and its properties were evaluated. PZT and SMA particle contents in the resin film were different, and the vibration damping changes according to the contents were observed and the tendency was analyzed. The carbon black particles were added to the resin film containing the PZT particles, and then the vibration damping change pattern was confirmed.

3.2. Particles dispersed resin film manufacturing process

Experiments were conducted to fabricate resin films containing PZT and SMA particles. The polymer resin used for the resin film is YD-128 of Kukdo Chemical. Resin films were made using the film casting equipment shown in Figure 19. First, PZT particles are added to the polymer resin. Then, the particles are evenly dispersed in the resin using a 3-roll-mill machine. The polymer resin in which the particles are dispersed is put into a vacuum oven and deformed. In order to confirm the productivity depending on the thickness of the resin film, resin film fabrication experiments were performed under the conditions of 100um, 60um, and 20um as shown in Table 1 above. The production process of the resin film is as follows. First, the resin containing the particles poured into the resin reservoir of the equipment. The PET film, which has been surface-treated so that it can be easily deformed, passes through the resin reservoir through the rollers. The resin-impregnated PET film passes through the blade controlling the thickness of the resin film, and the resin is applied on the PET film to a constant thickness as it passes through the blade. At this time, the productivity of the resin film depends on the conditions such as

viscosity, surface tension, and temperature of the resin. The PET film coated with the resin passes through a furnace, which can be heated according to the experimental conditions during transportation, and the heating conditions are not used in this experiment. As can be seen in Figure 20, the results of the experiments by film thickness are as follows. It can be seen that the film of 100um thickness is not coated well on the PET film due to the viscosity of the resin. In the case of a film with a thickness of 60 μm, although some coating is performed well, a large number of bubbles are generated and the non-uniformity of the composite material specimen is increased. The specimen with a thickness of 20 μm is very well coated on the PET film. In addition, since the size of particles used is less than 20μm, the thinner the film, the better the dispersion of the particles is expected. Considering the productivity of the film and the dispersion of the particles at the same time, it was judged that it would be best to use a film with a thickness of 20 μm for the experiment. Therefore, all subsequent experiments were carried out using 20μm resin films.

3.3. Specimen preparation

In order to apply the prepared particle-containing resin film to the carbon fiber-reinforced composite material, a method of directly transferring the resin

film to the prepreg was used. Since the PET film has been subjected to release treatment and the film is very thin, it can be easily transferred.

As shown in Table 2, the specimens were made as follows. Carbon fiber reinforced plastic composites were made of unidirectional carbon fiber prepreg by using hand layup and hot press method. Four sheets of prepreg were laminated with unidirectional (0° direction), and the PZT ceramic particles dispersed resin film were transferred in every interlayer. The amount of dispersed PZT particles in resin film varied from $0\,\mathrm{g}/m^2$ to $25\,\mathrm{g}/m^2$ in increments of $5\mathrm{g}/m^2$, therefore, six types of specimens were manufactured with 15 specimens in each type. Laminated prepreg was cured for 2hours, at the temperature of 130°C, and the pressure of 2.2bar using a hot-press. Specimens were produced according to the ASTM 5023 standard with 65mm in length, 13mm in width, and 0.6mm in thickness [8]. I made CFRP specimens with SMA particles dispersed resin film by following the same manufacturing process of composite materials with PZT particles. The loading of SMA particles in the resin film varied from $0\mathrm{g}/m^2$ to $25\mathrm{g}/m^2$ in increments of $5\mathrm{g}/m^2$. Six types of specimens were manufactured with 15 specimens in each type. CFRP specimens with PZT with carbon black particles were made by following the same manufacturing process of composite materials with PZT particles. The loading of carbon black 6 percent and 12 percent of PZT

dispersed in resin. Five types of specimens were manufactured with 5specimens in each type.

3.4. Experiments

SEM (Scanning electron microscope) images were used to evaluate the degree of dispersion of the prepared particle-containing resin films. The results are as follows in Figure 23, both SMA particles and PZT particles are uniformly distributed in the film. Since the SMA particles have a relatively smaller diameter than the PZT particles, the number of particles per unit area is larger for SMA. However, since both particles have no difference in density, the mass per unit area is the same.

The loss factor of particles dispersed composite specimens was measured by DMA.

3.5. Results

As shown in Figure 24, the loss factor of CFRP with PZT dispersed resin film results are presented. The amount of dispersed PZT particles in resin film varied from $0\mathrm{g}/m^2$ to $25\mathrm{g}/m^2$ in increments of $5\mathrm{g}/m^2$. The data for each point is the

average of $15\mathrm{g}/m^2$ specimen measurements. Neat specimens mean that has ho particles in linter laminar of CFRP. As the particle content increases, the measured loss factor value also increases. The frequency range in which the loss factor increases is about 100 Hz to 120 Hz. In the case of specimens in which particles were directly dispersed between the composite layers, the maximum value was observed at $15\mathrm{g}/m^2$, and thereafter, it tended to decrease. However, when resin film is used, an increase in loss factor can be observed at $20\mathrm{g}/m^2$. This confirmed the efficiency of resin film production. However, at 25, there is a tendency to decrease again. In spite of dispersing particles in resin film, excessive amount of the particles loading bad influence on dispersion.

As shown in Figure 24, the loss factor of CFRP with SMA dispersed resin film results are presented. The amount of dispersed SMA particles in resin film varied from $0\mathrm{g}/m^2$ to $25\mathrm{g}/m^2$ in increments of $5\mathrm{g}/m^2$. The data for each point is the average of $15\mathrm{g}/m^2$ specimen measurements. As the particle content increases, the measured loss factor value also increases. Unlike specimens with PZT particle dispersed resin film results, as expected, the frequency range in which the loss factor increases is about 50Hz to 100 Hz. In the case of specimens in which particles were directly dispersed between the composite layers, the maximum value was observed at $20\mathrm{g}/m^2$. Similar trends can be seen for specimens containing particles. However, the increase rate of

the loss factor is higher for resin film specimens. This is considered attributable to the result of increasing the degree of dispersion of the particles using the particles dispersed resin film. In order to confirm the increase of particle dispersion due to the use of the film, the cross section of the specimen was confirmed by EPMA (Electron probe micro analysis) and SEM (Scanning electron microscope). As shown in Figure 25, the lead element (Pb) contained in the PZT particles was traced and mapped using EPMA, and the particle dispersion effect due to the use of the film can be confirmed. However, as the content of the particles increases, the aggregation of the particles increases and the degree of dispersion decreases. SEM (Scanning electron microscope) shows the cross section of the specimen in Figure 26. It is confirmed that the increase in the content of the particles also has a bad influence on the degree of dispersion of the particles. The method of using the film rather than the conventional hand dispersing can disperse the particles better, but the aggregation due to the increase of the particle content is not eliminated.

The DMA results of the carbon fiber composite material including the SMA particles dispersed resin film and the DMA results of the carbon fiber composite material including the resin film in which the PZT particles dispersed are shown in Figure 27. It is clearly distinguished that the optimum frequency of the two materials is different. With reference to this result, CFRP specimens were

fabricated using resin films dispersed in PZT and SMA particles at the same time.

The DMA results of the carbon fiber composite material including the SMA and PZT mixed particles dispersed resin film are in Figure 28. The data for each point is the average of fifteen specimens' measurements. The partial content of each kind of particles in the mixture of SMA and PZT particles dispersed resin film is $10\mathrm{g}/m^2$. Therefore, Figure 28 shows the comparison of the loss factor values of $10\,\mathrm{g}/m^2$ composite specimens with PZT and SMA particles, respectively. The loss factor results of carbon fiber reinforced composite specimens containing resin films with SMA and PZT mixed particles were measured to be larger than the loss factor of neat specimens as a whole. Compared to the results of CFRP specimens made of resin films containing $10\mathrm{g}/m^2$ SMA particles, we found that SMA has a very large effect on the frequency range. However, when compared with the results of the CFRP specimen made of resin film containing $10\mathrm{g}/m^2$ PZT particles alone, the increase is small amount. The thermal energy generated from the deformation of the piezoelectric material accelerates the phase change of the shape memory alloy when the piezoelectric material and the shape memory alloy are simultaneously applied.

The DMA results of the CFRP specimens with PZT with carbon black

particles dispersed resin film are in Figure 29. The data for each point is the average of fifteen specimens' measurements. The loss factor of CFRP specimens with loading of carbon black 6 percent by weight and 12percent by weight of PZT dispersed in resin and the loss factor of CFRP specimen made of resin film containing $20\mathrm{g}/m^2$ PZT particles alone is shown in Figure 29. Compared with the results of specimens containing only PZT, the loss factor of the carbon black mixed with 6% of the PZT particle weight increased more. In addition, the frequency range in which the vibration damping effect shifted forward with the largest amount. The loss factor of the carbon black mixed with 12% of the PZT particle weight did not increase much more than the loss factor of the PZT-only specimen. In this case, the frequency range in which the vibration damping effect is the largest shifted further forward. This is presumably due to the change in the electrical conductivity of the matrix by mixing carbon black.

The DMA results of the CFRP specimens with PZT with various particles size are in Figure 30. Three types of particles were prepared. Particles with a grid size of 10 um, 20 um, and 25 um were filtered out. Three kinds of particles were obtained from them, 10um or less, 10um or more and 20um or less, and 25um or more. Three kinds of particles were fabricated as resin films and the specimens were applied to CFRP to measure the loss factor. Experimental

results show that there is no significant tendency of variation of vibration damping due to particle size. According to Uchino [6], it is known that the magnitude of the piezoelectric effect varies with the particle size of the PZT ceramics. However, this refers to the grain size of the grain. In this experiment, the size of the grain size is determined because the prefabricated piezoelectric ceramic plate is crushed and used. Since grain size does not vary, the effect of size in this experiment is influenced by aggregation. It is expected that results that are more accurate can be obtained by fabricating piezoelectric ceramics particles with grain sizes different from each other.

3.6. Summary

In this chapter, we have fabricated a thin resin film adding particles for efficiently dispersing PZT particles and SMA particles in a composite material. In addition, vibration damping characteristics were measured and analyzed by placing a resin film with particles of various conditions between carbon fiber composite material layers. As a result, it confirmed that the PZT particles had a greater vibration damping effect when they were well dispersed. However, this can be a disadvantage when it is present inside the PZT particle composite material in an amount more than a certain amount, irrespective of the dispersion.

In the case of SMA, we also confirmed that the vibration damping effect increases when the particles are well dispersed. In addition, it confirmed that the range of the frequency at which the vibration damping increase effect of PZT and SMA becomes maximum is different from each other. It is found that the vibration damping of PZT and SMA applied specimens is different from the conventional one. In order to increase the vibration damping due to the electric effect of the PZT particles, experiments were conducted in which the conductivity of the resin film was increased by using carbon black. As a result, it confirmed that when the electrical conductivity of the resin film was high, the vibration damping effect by the PZT particles was increased.

Chapter 4. Computational analysis

4.1. Overview

Throughout the previous chapters, the vibration damping of composite materials containing PZT and SMA particles was experimentally analyzed. The experimental data are used to analyze various parameters such as particle size, and conductivity of the matrix. In addition, they are compared with experimental data to establish a rough reference for vibration damping mechanism. For the sake of simplicity, the carbon fiber and polymer matrix are assumed one conductive matrix in the analytical model. The piezoelectric circuit between matrix and a particle is modeled similar to the RC circuit. The analysis of the vibration damping by the dissipation of energy due to cyclic loading is as follows.

First, for a matrix containing a spherical particle, which have piezoelectric property, the effective properties measured from the mechanical model using Abaqus.

Second, stress and energy distribution calculations are performed on the shape of the specimen using the effective properties.

Third, the results are used to calculate various parameters such as volume fraction, size, and electrical conductivity of the matrix.

Through the above process, the validity of the prediction of the vibration damping performance of the specimen using the numerical analysis is examined and the reliability of the experimental results is confirmed.

4.2. Theoretical backgrounds

4.2.1. Piezoelectric constitutive equation

In general, poled piezoelectric ceramics are transversely isotropic materials. To be in agreement with the IEEE Standard on Piezoelectricity [24], the isotropic plane is defined as the xy-plane. The piezoelectric material therefore exhibits symmetry about the z-axis, which means the poling axis of the material. Consider the tensor representation of the strain–electric displacement form [24] where the independent variables are the stress components and the electric field components:

$$\mathrm{S}_{ij} = S^{E}_{ijkl}\mathrm{T}_{kl} + D_{kij}E_k \tag{4.1}$$

$$\mathrm{D}_i = d_{ikl}T_{kl} + \varepsilon^{T}_{ik}E_k \tag{4.2}$$

The field variables are the stress components(T_{ij}), strain components(S_{ij}), electric field components(E_k), and the electric displacement components($D_{k)}$. The standard form of the piezoelectric constitutive equations can be given in four different forms by taking either two of the four field variables as the independent variables. It is the preferred form of piezoelectric configuration basic equation for the boundary media (which is to remove a portion of the stress component, which depends on the geometry and the electric field component part according to the arrangement of the electrodes). Equations (4.1) and (4.2) can be given in matrix form as

$$\begin{bmatrix} S \\ D \end{bmatrix} = \begin{bmatrix} s^E & d^t \\ d & \varepsilon^T \end{bmatrix} \begin{bmatrix} T \\ E \end{bmatrix} \tag{4.3}$$

The superscripts E and T indicate that the constants are evaluated at constant electric field and constant stress, respectively, and the superscript t denotes transpose.

The expanded form of Equation (4.3) is

$$\begin{bmatrix} S_1 \\ S_2 \\ S_3 \\ S_4 \\ S_5 \\ S_6 \\ D_1 \\ D_2 \\ D_3 \end{bmatrix} = \begin{bmatrix} s_{11}^E & s_{12}^E & s_{13}^E & 0 & 0 & 0 & 0 & 0 & d_{31} \\ s_{12}^E & s_{11}^E & s_{13}^E & 0 & 0 & 0 & 0 & 0 & d_{31} \\ s_{13}^E & s_{13}^E & s_{33}^E & 0 & 0 & 0 & 0 & 0 & d_{33} \\ 0 & 0 & 0 & s_{55}^E & 0 & 0 & 0 & d_{15} & 0 \\ 0 & 0 & 0 & 0 & s_{55}^E & 0 & d_{15} & 0 & 0 \\ 0 & 0 & 0 & 0 & 0 & s_{66}^E & 0 & 0 & 0 \\ 0 & 0 & 0 & 0 & d_{15} & 0 & \varepsilon_{11}^T & 0 & 0 \\ 0 & 0 & 0 & d_{15} & 0 & 0 & 0 & \varepsilon_{11}^T & 0 \\ d_{31} & d_{31} & d_{33} & 0 & 0 & 0 & 0 & 0 & \varepsilon_{33}^T \end{bmatrix} \begin{bmatrix} T_1 \\ T_2 \\ T_3 \\ T_4 \\ T_5 \\ T_6 \\ E_1 \\ E_2 \\ E_3 \end{bmatrix} \quad (4.4)$$

Where the contracted notation (i.e., Voigt notation: 11 → 1, 22 → 2, 33 → 3, 23 → 4, 13 → 5, 12 → 6) is used so that the vectors of strain and stress components are

$$\begin{bmatrix} S_1 \\ S_2 \\ S_3 \\ S_4 \\ S_5 \\ S_6 \end{bmatrix} = \begin{bmatrix} S_{11} \\ S_{22} \\ S_{33} \\ 2S_{23} \\ 2S_{13} \\ 2S_{12} \end{bmatrix}, \begin{bmatrix} T_1 \\ T_2 \\ T_3 \\ T_4 \\ T_5 \\ T_6 \end{bmatrix} = \begin{bmatrix} T_{11} \\ T_{22} \\ T_{33} \\ T_{23} \\ T_{13} \\ T_{12} \end{bmatrix} \quad (4.5)$$

Therefore, the shear strain components in the contracted notation are the engineering shear strains. It should be noted from the elastic, piezoelectric, and dielectric constants in Equation (4.4) that the symmetries of transversely isotropic material behavior ($s_{11}^E = s_{22}^E$, $d_{31} = d_{32}$, etc.) are directly applied.

4.2.2. SMA hyperelasticity

SMA exhibits hyperelastic hysteresis with no permanent deformation, but permanent deformation is maintained even if the external force is removed beyond the elastic limit. The characteristics of SMA are inelasticity by heating, thereby exhibiting shape recovery effect and generating shape elasticity. The shape restoring force generated at this time is about 5 times the force at the time of deformation.

4.2.3. Dynamic properties in linear viscoelasticity [26]

When a specimen, which had viscoelastic property, is loaded by uniaxial cyclic displacement $\varepsilon^*(t)$ with amplitude ε_0 and angular velocity ω, $\varepsilon^*(t)$ represented as follows,

$$\varepsilon^*(t) = \varepsilon_0 e^{i\omega t} \tag{4.6}$$

Based on the theory of linear viscoelasticity, the output stress σ^* represented as follows,

$$\sigma^* = E^*(\omega)\varepsilon^*(t) \tag{4.7}$$

$E^*(\omega)$ is the complex modulus is represented as follows,

$$E^*(\omega) = E'(\omega) + iE''(\omega) \tag{4.8}$$

$E'(\omega)$ is the storage modulus and $E''(\omega)$ is the loss modulus. The phase shift angle δ between input strain and output stress (or vice versa) calculated as,

$$\tan\delta = E^{"}/E' \tag{4.9}$$

Hereby, the energy consumed during one cycle($\tau = 2\pi/\omega$), ΔW is calculated. The real part of input strain of equation (4.7) represented as

$$\varepsilon(t) = \mathrm{Re}[\varepsilon^*(t)] = \varepsilon_0 cos\omega t \tag{4.10}$$

Thus, output stress, which corresponds to strain, represented as,

$$\sigma(t) = \mathrm{Re}[E^*(\omega)\varepsilon(\omega)] = \varepsilon_0(E' cos\omega t - E^{"} cos\omega t) \tag{4.11}$$

The energy ΔW consumed during a cycle of load calculated as follow,

$$\Delta W = \int_0^{\tau} \sigma(t)\frac{d\varepsilon}{dt}dt = \pi E^{"}\varepsilon_0^2 \tag{4.12}$$

When a material undergoes a cycle, it loses energy by ΔW, and some part of it dissipates into heat.

4.2.4. Shunted piezoelectric material modeling

Looking out through the piezoelectric constitutive equation in advance can be seen to think of the material of the piezoelectric electro-mechanical coupling factor. The meaning of the electro-mechanical coupling factor is as follows:

k^2= ($Stored\ electrical\ energy$ / $input\ mechanical\ energy$)

=($Stored\ mechanical\ energy$ / $input\ electrical\ energy$)

It can also be expressed as:

$$U_E(electrical\ energy) =$$

$$U_m(mechanical\ energy) \times k^2$$

Therefore, k^2 is also used as an index of the performance of the piezoelectric material. We have previously proposed that a Shunted piezoelectric material model can be assumed a circuit model with similarities to RC circuits. The following Figure 31 shows a better understanding.

When the attenuation factor of the piezoelectric shunted circuit calculated by the RC circuit model may represent the attenuation factor η by electro-mechanical coupling factor [25]. The η value is the maximum loss factor when the shunted PZT material is assumed an RC circuit.

$$\eta = \frac{k_{ij}^2 \Omega_0}{1 - k_{ij}^2 + \Omega_0^2} \tag{4.13}$$

$$\Omega_0 = RC\left(1 - k_{ij}^2\right)\omega \tag{4.14}$$

$$C = A\varepsilon_3^T / t \tag{4.15}$$

$$k_{ij} = \frac{d_{ij}}{\sqrt{s_{jj}^E \varepsilon_i^T}} \tag{4.16}$$

The variables are the loss factor for shunted piezoelectric material(η), the frequency(ω), the capacitance of PZT(C), the resistance(R), the Piezoelectric coefficient(d_{ij}), the permittivity (ε_i^T), the electro-mechanical coupling factor

(k_{ij}), and the compliance (S_{jj}^{E})

The simulation goal in this chapter is to obtain the effective value of the above values and then calculate the vibration damping nu value through the result.

4.3. Simulation condition

The matrix and the particle determine the piezoelectric effective properties in a composite. In this simulation, it is assumed that PZT is distributed in the matrix very uniformly as a sphere-shaped particle, and prepreg of epoxy and carbon fiber is used as the matrix. The properties of the materials used for modeling are as follows in Table 3. Since the shape of the PZT contained in the composite is spherical and the distribution is assumed uniform, it can be assumed that the PZT particle sphere is contained in the simple cubic as shown in Figure 32 and 33.

PZT particles are assumed to be poled in the Z direction. In this analysis, ABAQUS was used to calculate the 3D solid element. Figure 33 shows the particles in the composite lattice at ABAQUS. The above elements have displacement and electrical potentials, respectively. To calculate effective properties in the composite, the electrical potential was applied to the upper

element in the Z direction, which is the poling direction, and the size was set to 1000V. On the opposite surface, a boundary condition is applied to the electrical potential and displacement to zero. As a result, the electrical and mechanical displacement or strain due to applied electrical potential are calculated.

4.4. Results

As the result of imposing the electrical potential in the poling direction of the PZT used in the analysis, the displacement of the element in the z direction was observed. The results are as follows in Figure 33. Constraints were applied to the surface of each part so that PZT and matrix were not separated during displacement by applying electrical potential. In order to improve the damping effect through the piezoelectric element, a strain is generated for an applied stress, and since the strain is converted into an electrical signal to be emitted as thermal energy. Since the damping effect of the composite material can be affected by the ratio of the piezoelectric elements and the particle volume fraction, the volume fraction can be controlled through the values of d and x, and the d value can be derived from the calculated values using ABAQUS.

As shown in Figure 34, it represented the relation between effective piezoelectric coefficient and the particle volume fraction. As the particle volume fraction increased,

effective piezoelectric coefficient, which means the piezoelectric effect of the whole matrix containing the particles, increased. This is because the fraction of the piezoelectric material in the matrix becomes larger.

As shown in Figure 35, it represented the relation between effective compliant coefficient and the particle volume fraction. As the particle volume fraction increased, effective compliant coefficient of material decreased. Since the stiffness of PZT particles is very large compared to the matrix, the compliant of the whole model tends to decrease as the fraction of particles increases.

As shown in Figure 36, it represented the relation between effective dielectric constant and the particle volume fraction. As the particle volume fraction increased, effective dielectric constant increased.

Based on the above values and Equation 4.16, the relation between effective piezoelectric coupling coefficient and the particle volume fraction can be calculated. The calculation results are shown in Figure 37. The electro-mechanical coupling factor increases as the particle content increases, and then decreases again at some point. Although many conditions are limited and differ from actual experiments, the electro-mechanical coupling factor is a very important factor in the shunted piezoelectric vibration damping mechanism.

From the above results and equation 4.13, we have calculated the loss factor η of the model. The results are shown in Figure 38. The η values are calculated according to three frequencies of 100 Hz, 110 Hz, and 120 Hz. As can be seen

from the results, the loss factor tends to increase as the fraction of particles increases. This tendency is similar to that of the experiment, but it is very low for absolute values. This is an error caused by assuming that RC value is not appropriate in the calculation model. The appropriate RC value needed in equation 4.13 should be obtained throughout accurate calculations later.

Chapter 5. Conclusion

In this study, SMA powder dispersed between PZT (lead zirconate titanate) ceramic particles, carbon fiber and epoxy matrix was used to make CFRP composites with high damping performance. The loss factor (tan δ) is measured using a dynamic mechanical analyzer (DMA) to determine structural changes in vibration damping.

In Chapter 2, PZT ceramic particles were prepared by dispersing carbon fiber reinforced composites in order to improve vibration damping performance of carbon fiber reinforced composites. In order to confirm the effect of piezoelectric effect on the increase of vibration damping by using TiO2 particles without piezoelectric effect, the same experiment was carried out with the same method. Because of the experiment, the addition of PZT ceramic particles improves the vibration damping performance of the carbon fiber reinforced composite material. Increasing the PZT load until a certain amount of PZT ceramic particles is loaded increases the vibration damping force. However, loading a certain amount of PZT does not increase the vibration damping force but rather reduces it. The experimental results of CFRP using TiO_2 particles were different from those of PZT. In the PZT experiment, the optimum value of the load exists. However, the experimental results of CFRP

using TiO_2 particles do not have optimum loading values. This means that the two materials act as different mechanisms to increase vibration damping. To improve the vibration damping force of CFRP, carbon fiber reinforced plastic (CFRP) composites using lead zirconate titanate (PZT) particles and shape memory alloy (SMA) were fabricated. The loss factor (tan δ) is measured using a dynamic mechanical analyzer (DMA) to determine the viscoelastic behavior of the material. Both materials have the effect of increasing the damping force of CFRP vibration, but the energy dissipation mechanism of each material is different. Therefore, there is a difference in optimum load and vibration frequency. Based on the results, we expect carbon fiber reinforced plastic composites containing PZT and SMA to have better damping performance.

In Chapter 3, we made thin resin films using particles to efficiently disperse PZT particles and SMA particles into a composite material. In addition, vibration damping characteristics were measured and analyzed by placing a resin film having particles of various conditions between carbon fiber composite material layers. As a result, it was confirmed that the PZT particles have a larger vibration damping effect when they are dispersed well. However, it may be disadvantageous if a certain amount or more is present in the PZT particle composite material regardless of dispersion. In the case of SMA, it has been found that the vibration damping effect increases when particles are well

dispersed. In addition, it was confirmed that the range of the frequency at which the effect of increasing vibration damping of PZT and SMA becomes maximum is different from each other. It can be seen that the vibration damping of the PZT and SMA application specimens is different from the conventional one. In order to increase the vibration damping due to the electrical effect of the PZT particles, experiments were conducted to increase the conductivity of the resin film using carbon black. As a result, it was confirmed that when the electrical conductivity of the resin film is high, the effect of vibration damping by PZT particles is increased.

In chapter 4, we assumes a complex system in which lead zirconate titanate (PZT) ceramic particles, one of the most common piezoelectric materials, are applied to the CFRP manufacturing process. It is based on the potential of the composite material modeled using ABAQUS. Displacement and mechanical deformation have been calculated. The effective piezoelectric properties of the composite material containing PZT particles were determined. Compares the calculated results to the analysis solution to find the problem and perform the supplemental analysis.

References

[1] Nielson, L. E., [Mechanical properties of polymer and composites] New York, Marcel Dekker (1974)

[2] Song, G., Qiao, P., Binienda, W., Zou, G., "Active Vibration Damping of Composite Beam using Smart Sensors and Actuators." J. Aerosp. Eng., 3(97), 97-103 (2002)

[3] Rao, M. D., Echempati, R., Nadella, S., "Dynamic analysis and damping of composite structures embedded with viscoelastic layers" Compos Part B-Eng, 28(5), 547–554 (1997)

[4] Zhou, X., Shin. E., Wang, K.W., Bakis CE. "Interfacial damping characteristics of carbon nanotube-based composites" Compos Sci Technol, 64, 2425–37 (2004)

[5] Kim, S.Y., Tanimoto, T., Uchino, K., Nam, C. H., Nam, S., Lee, W. I., "Effects of PZT particle-enhanced ply interfaces on the vibration damping behavior of CFRP composites" Compos Part A-Appl S, 42, 1477-1482 (2011)

[6] Uchino, K., Ishii, T., “Mechanical damper using piezoelectric ceramics” J Ceram Soc Jpn, 96, 863–7 (1988)

[7] de Araújo, C.J., Rodrigues, L.F.A., Coutinho Neto, J.F., Reis, R.P.B., "Fabrication and static characterization of carbon-fiber-reinforced polymers with embedded NiTi shape memory wire actuators" Smart Mater Struct, 17, 65004 (2008)

[8] ASTM., “Standard test method for plastics: dynamic mechanical properties. In: Flexure (three point bending)” D 5023, ASTM International (2007)

[9] Uchino, K., [Ferroelectric devices] New York, Marcel Dekker (2000).

[10]Schueler R, Joshi SP, Schulte K. Damage detection in CFRP by electrical conductivity mapping. Compos Sci Technol 2001;921-30

[11]Dimitris C. Lagoudas., [Shape memory alloy: Modeling and Engineering Application], Springer(2007).

[12] C. M. Jackson, H. J. Wagner, R. J. Wasilewski, 55-Nitinol—The alloy with a memory: Its physical metallurgy, properties and applications, Tech. Rep. NASA SP-5110, NASA technology Utilization Office, Washington, D.C.

(1972).

[13] T. Duerig, K. Melton, D. Stockel, C. Wayman (Eds.), Engineering Aspects of Shape Memory Alloys, Butterworth-Heinemann, London, 1990.

[14]TA Instruments, “Q800 clamp specification”

, http://www.tainstruments.com/product.aspx?siteid=11&id=25&n=3

[15] Otsuka, Kazuhiro, and Clarence Marvin Wayman, eds. Shape memory materials. Cambridge University Press, 1999.

[16] Pérez-Sáez, R. B., et al. "Anelastic contributions and transformed volume fraction during thermoelastic martensitic transformations." Physical Review B 57.10 (1998): 5684.

[17] Van Humbeeck, Jan. "Damping capacity of thermoelastic martensite in shape memory alloys." Journal of Alloys and Compounds 355.1 (2003): 58-64.

[18] C. Poizat , M. Sester, “Effective properties of composites with embedded piezoelectric fibres”, Computational Materials Science 16 (1999) 89-97

[19] C.H. Zhang , Z. Hua, G. Gao, S. Zhao, Y.D. Huang., “Damping behavior and acoustic performance of polyurethane/lead zirconate

titanate ceramic composites" Materials and Design 46 (2013) 503–510

[20] G. Zhang, M.S. Wu, "Connectivity and shape effects on the effective properties of piezoelectric–polymeric composites", International Journal of Engineering Science 48 (2010) 37–51

[21] Suarez SA, Gibson RF, Sun CT, Chaturvedi SK. "The influence of fiber length and fiber orientation on damping and stiffness of polymer composite materials". Exp Mech 1986; 26(2):175–84.

[22] Hori M, Aoki T, Ohira Y, Yano S. "New type of mechanical damping composites composed of piezoelectric ceramics, carbon black and epoxy resin". Compos Part A-Appl S 2001;32:287–90

[23] Tian S, Cui F, Wang X. "New type of piezo-damping epoxy-matrix composites with multi-walled carbon nanotubes and lead zirconate titanate". Materials Letters 2008;62;3859–3861

[24] IEEE Standard on Piezoelectricity, (IEEE Standard 176-1987); Institute of Electrical and Electronic Engineers, 345 East 47th St, New York, NY 10017. Engineers, 345 East 47th St, New York, NY 10017.

[25] Hongming Z, Xiadong H, Fan Y, Lifeng H, Zhonghia X, Rongguo W. "Piezoelectric Modal Damping Performance of 0-3 piezoelectric Composite With Conducting Phase: Numerical Analysis and Experiments". Polymers & Polymer Composites, Vol. 22, No. 3, 2014

[26] J.OHNO, J.GOTOH, M.OKADA, M.Takashi, and S.Miwa "A Temperature Rise by Heat Generation on Viscoelastic Body under Periodic Load". Transaction of JSME Ser.A, 63(610), 1260-1265, (1997)

Figures

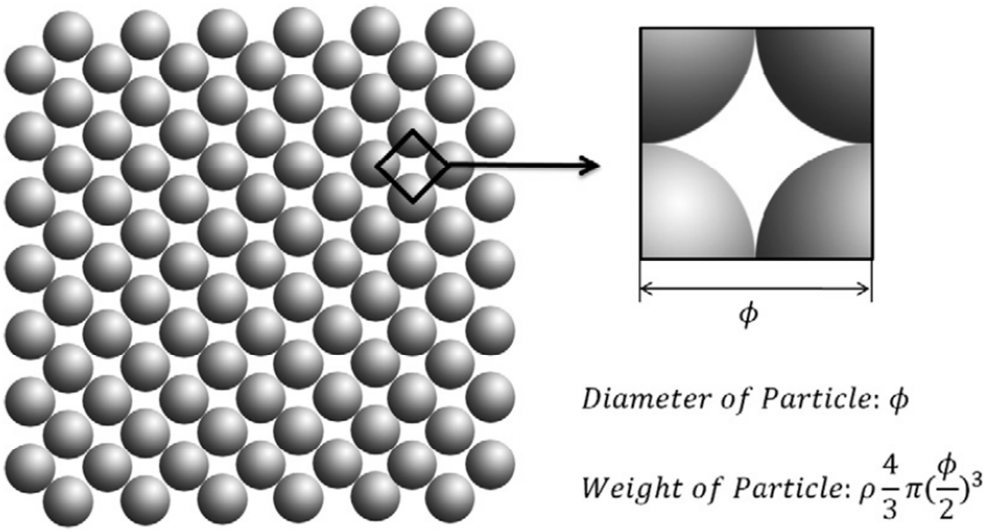

Figure 1. Scheme of optimum particles disperse in CFRP [5]

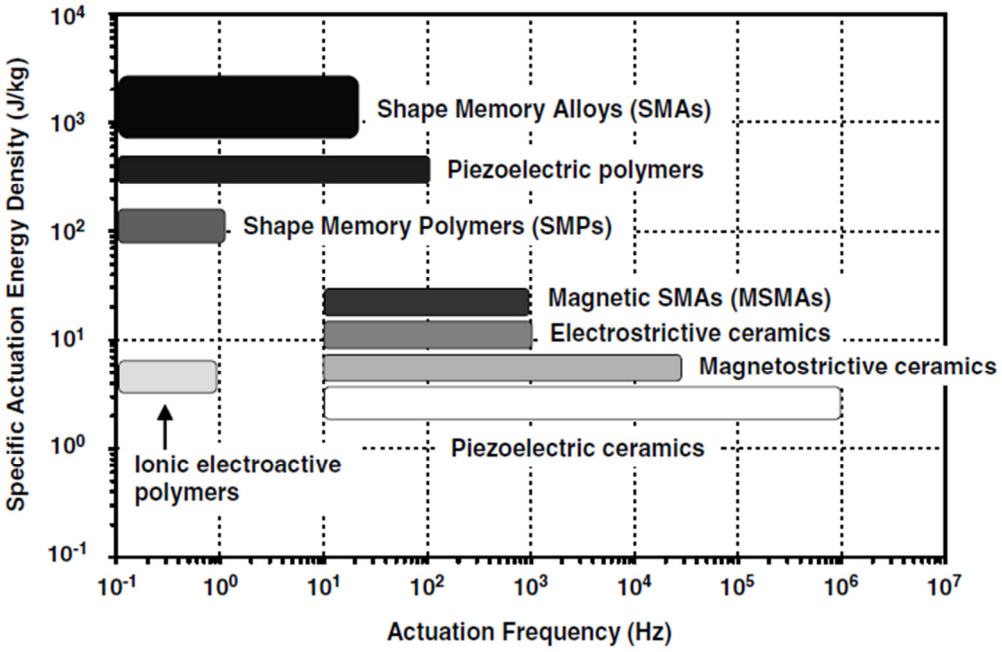

Figure 2. Actuation frequency diagram comparing the actuation frequency ranges of different active materials that exhibit direct coupling [11]

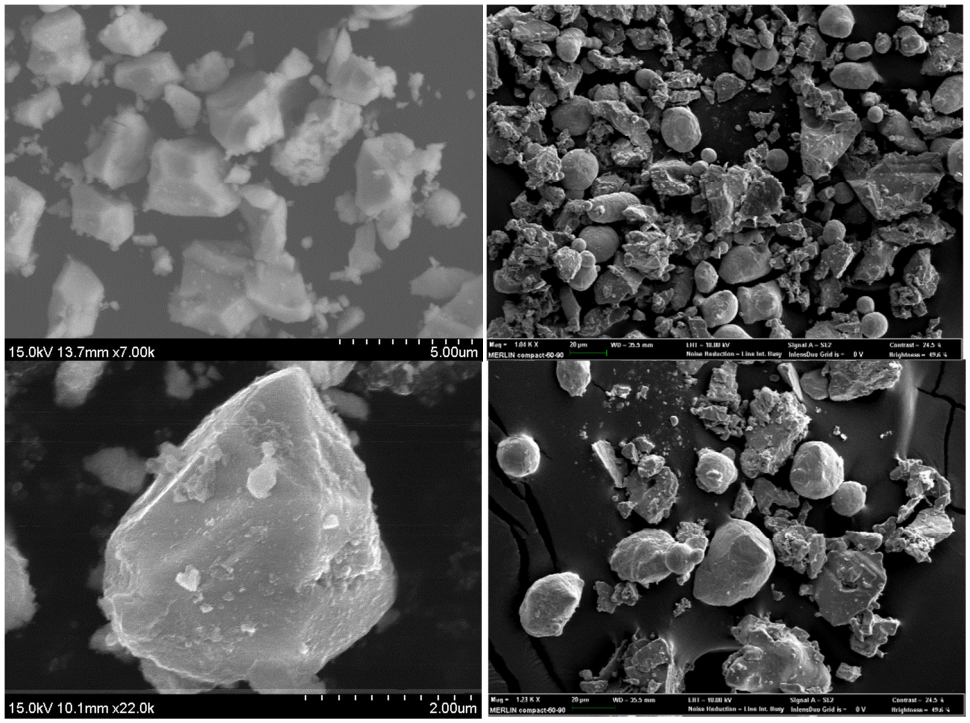

Figure 3. SEM image of PZT particles (Left) and SMA powder (Right)

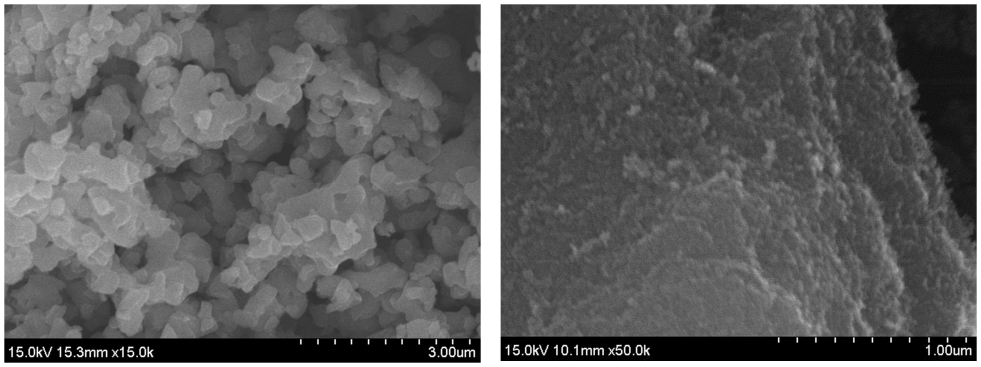

Figure 4. SEM image of TiO_2 particles (Left) and Carbon black (Right)

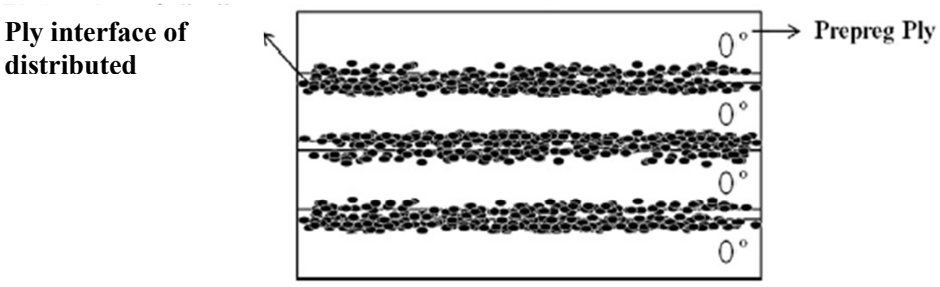

Figure 5. Scheme of carbon fiber reinforced plastic specimen with particles.

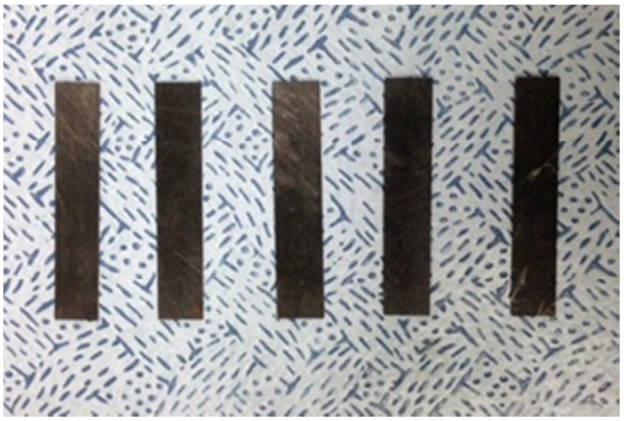

Figure 6. Image of specimens produced according to the ASTM 5023 standard with 65mm in length, 13mm in width, and 0.6mm in thickness.

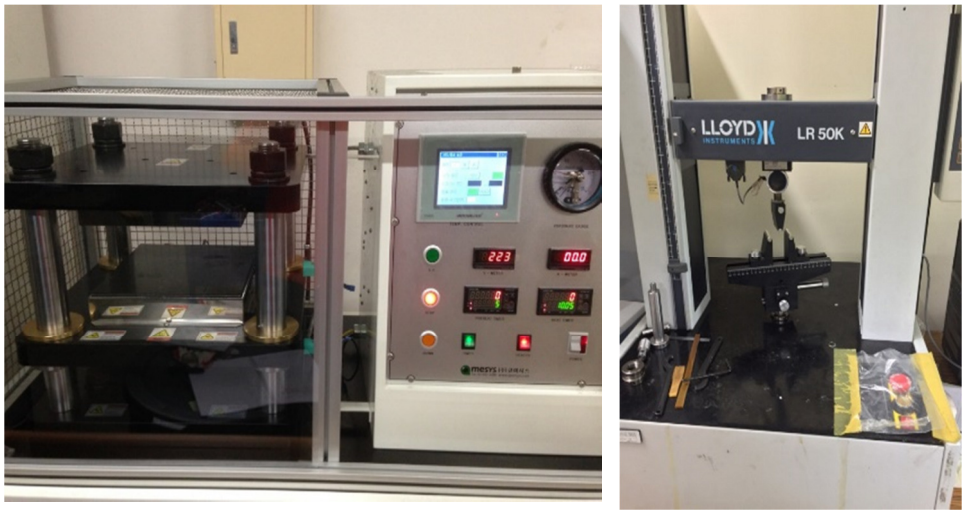

Figure 7. Image of hot press (Left) and Universal testing machine (UTM) (Right)

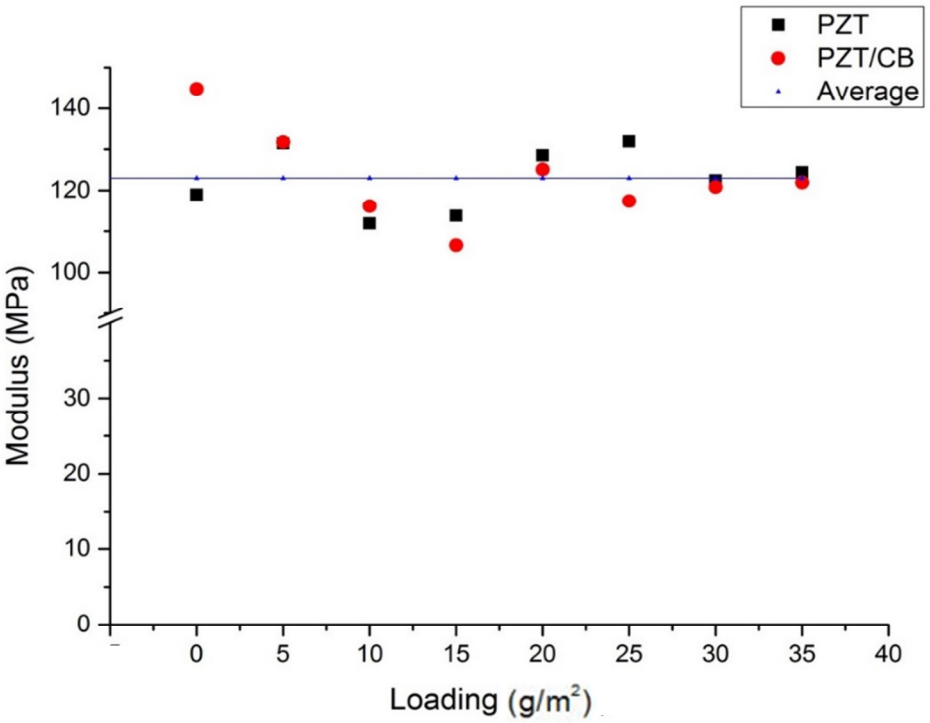

Figure 8. Flexural modulus test results according to filler particle type and its content

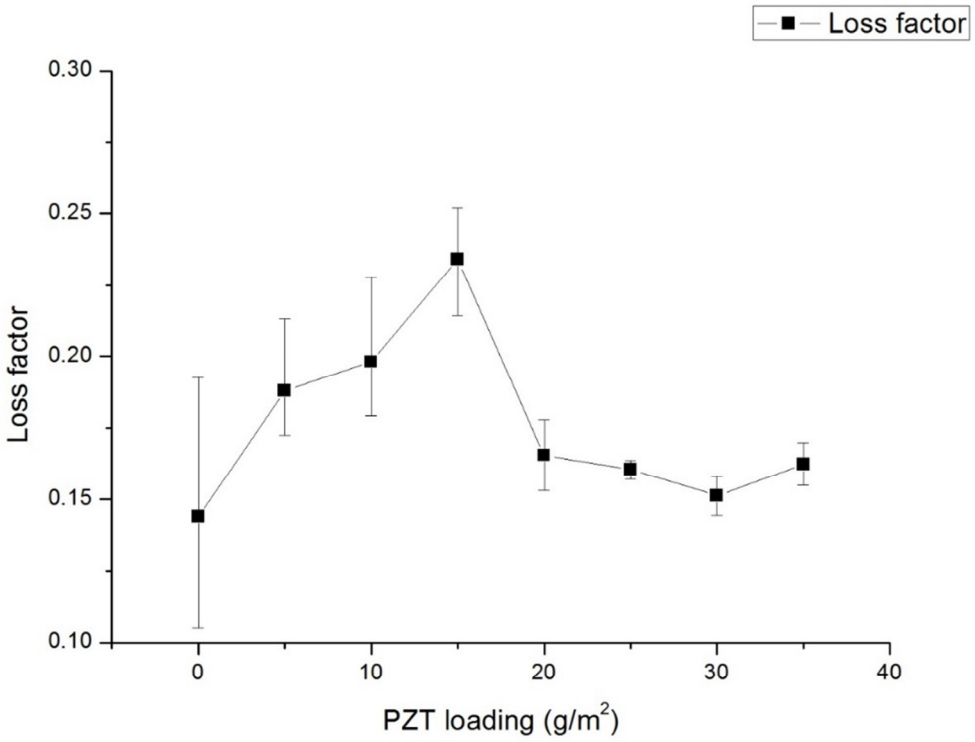

Figure 9. The loss factor of CFRP with PZT ceramic particles at 120Hz according to PZT particles loading

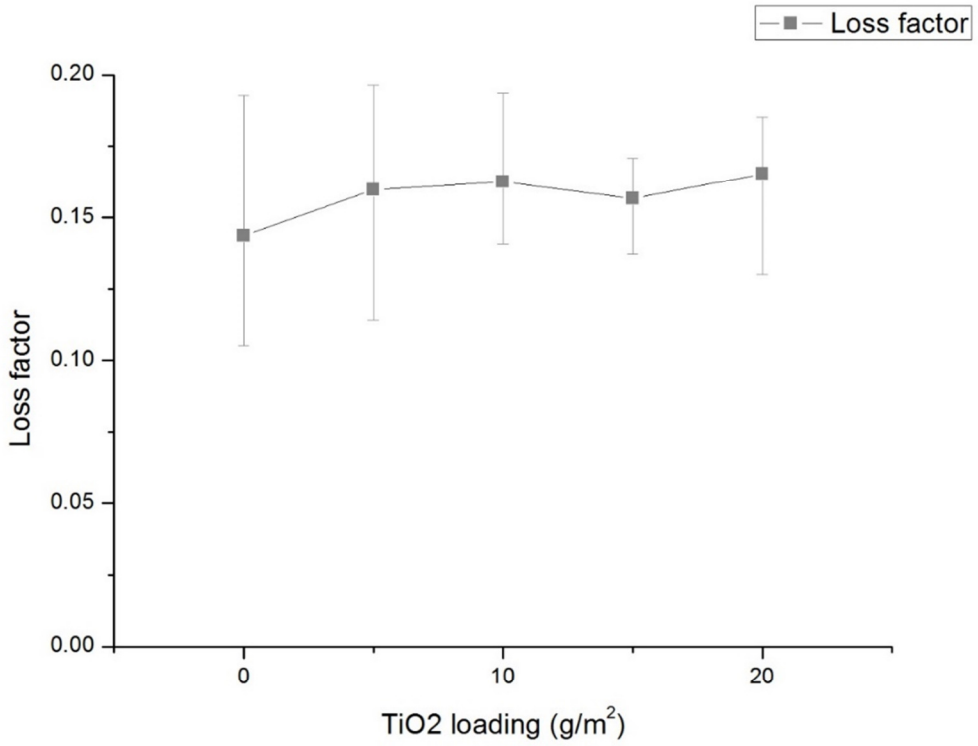

Figure 10. The loss factor of CFRP with TiO_2 particles at 120Hz according to TiO_2 particles loading

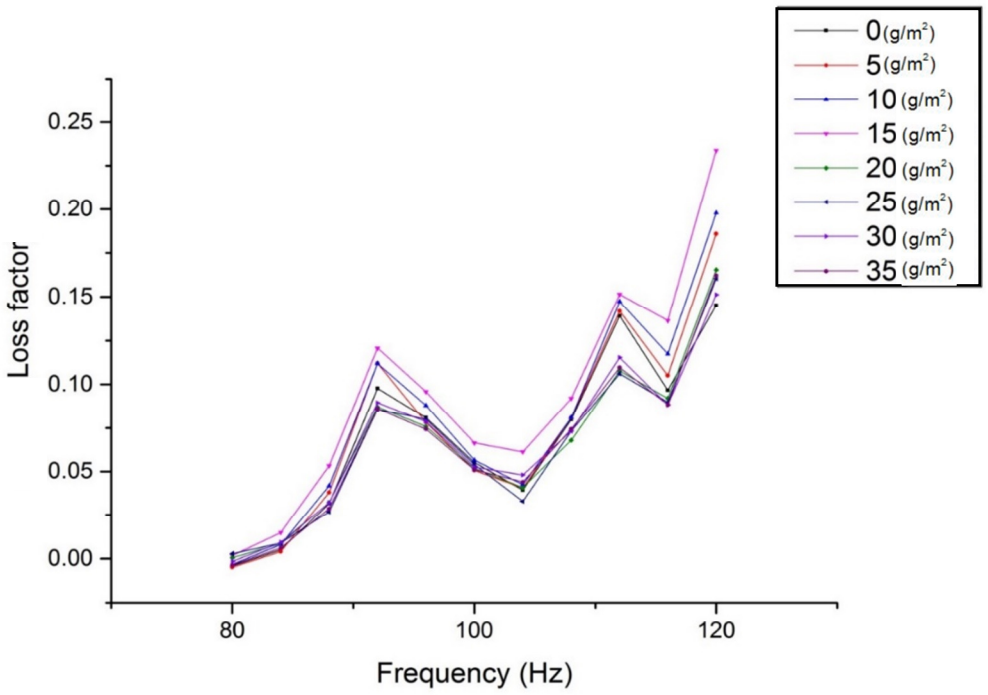

Figure 11. The change of loss factor along with frequency sweep and PZT particles loading

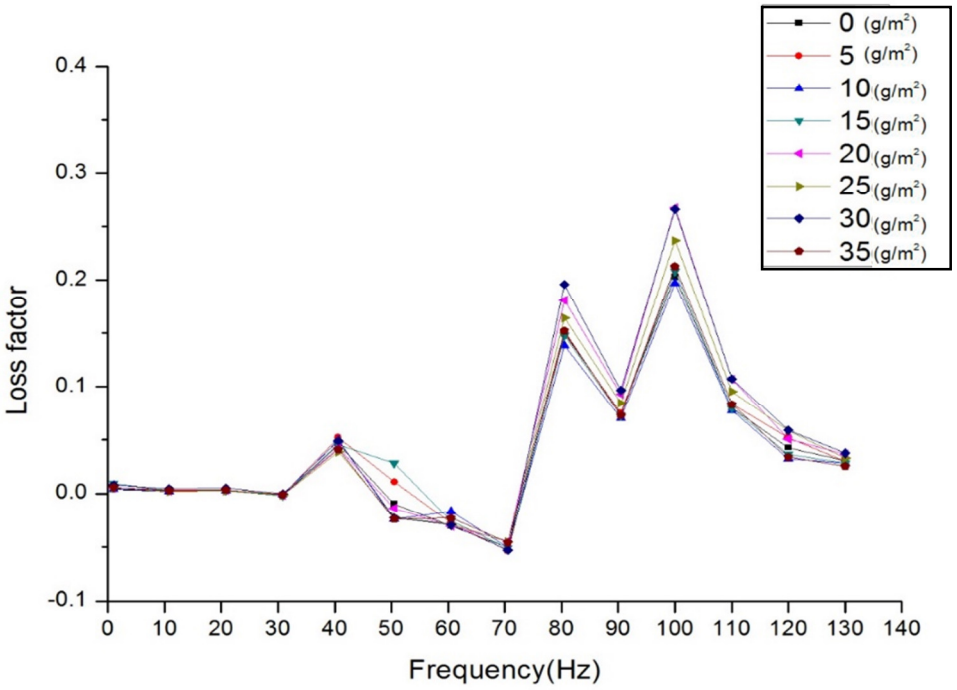

Figure 12. The change of loss factor along with frequency sweep and SMA particles loading

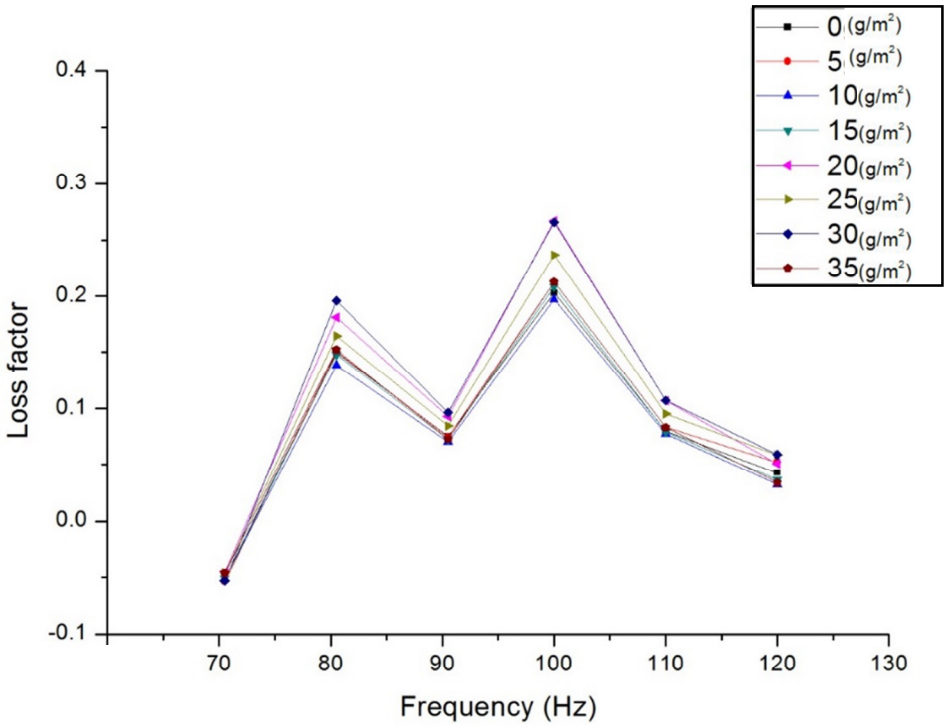

Figure 13. The change of loss factor along with SMA particles loading between 70 to 120 Hz

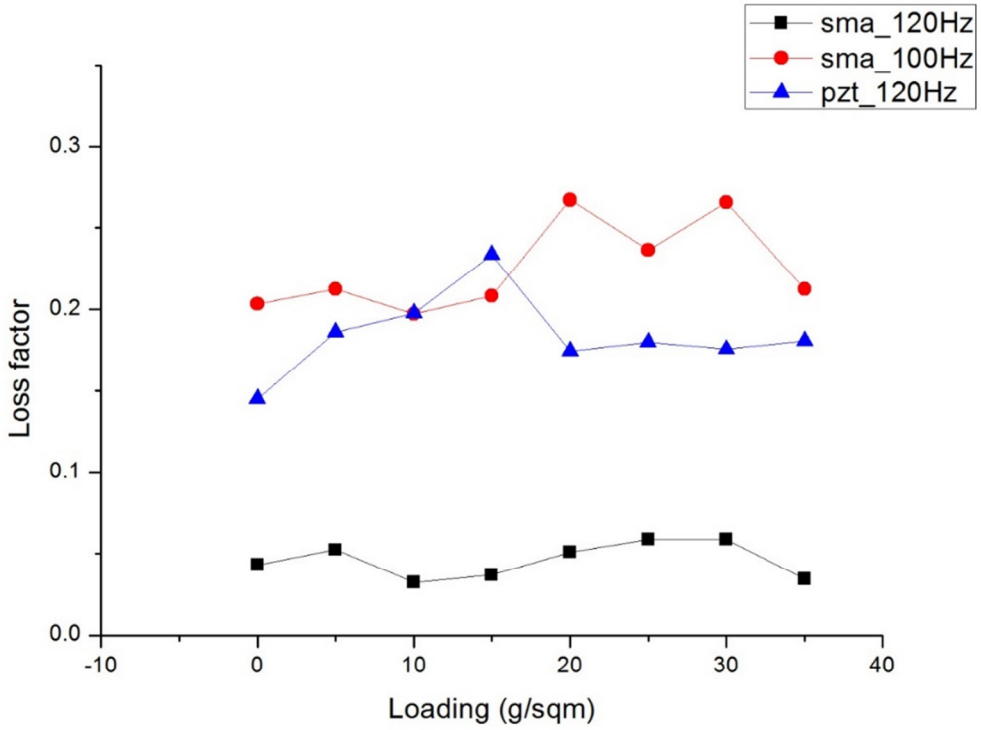

Figure 14. The loss factor of CFRP with PZT particles and SMA powder varied with loading at specific frequency (100Hz and 120Hz)

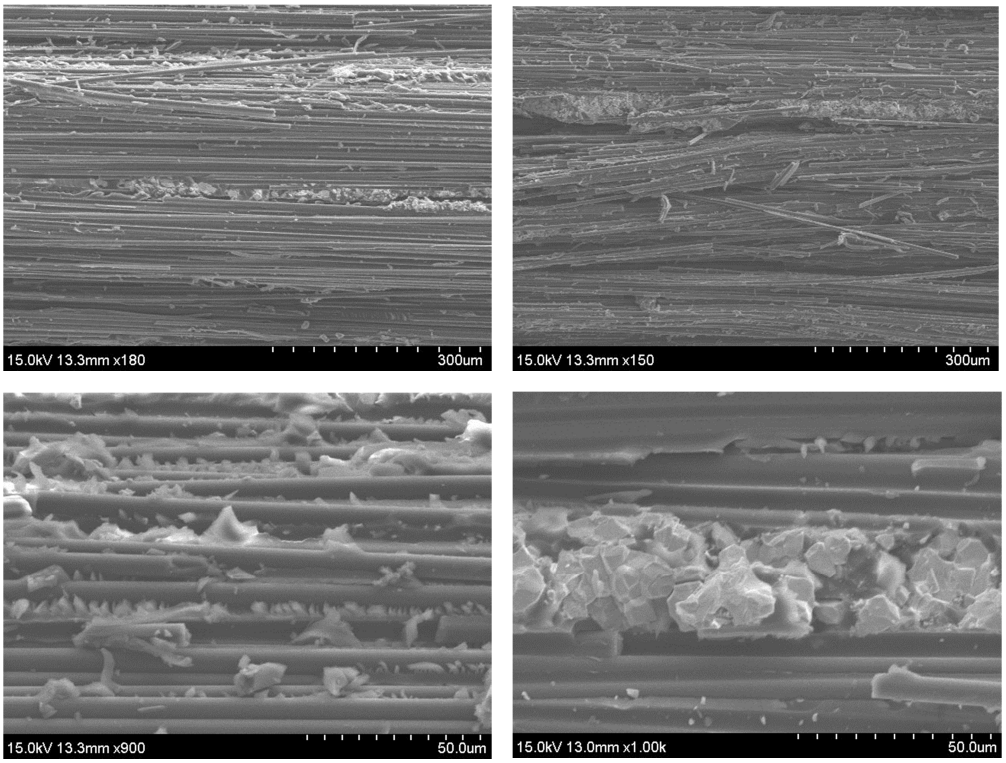

Figure 15. SEM image of CFRP cross section with 25 g/m^2 loading PZT

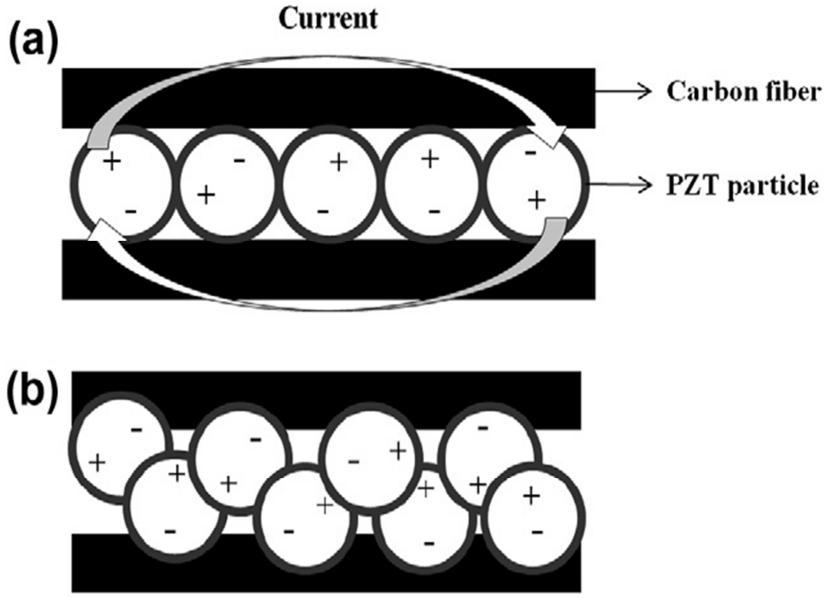

Figure 16. (a) Current is generated if the PZT particles are connected on both sides of the carbon fibers. (b) If the particles are overloaded, incomplete connectivity is created between the particles and carbon fibers, which inhibit the generation of current. [6]

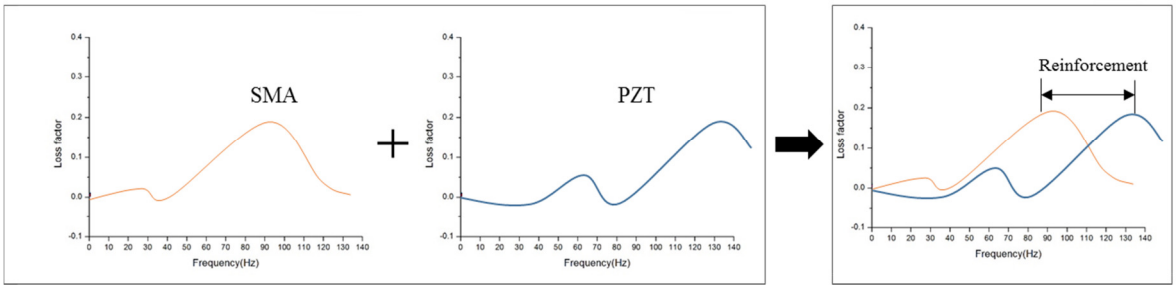

Figure 17. Scheme of Predicted changes in loss factor of composite materials using PZT and SMA particles simultaneously

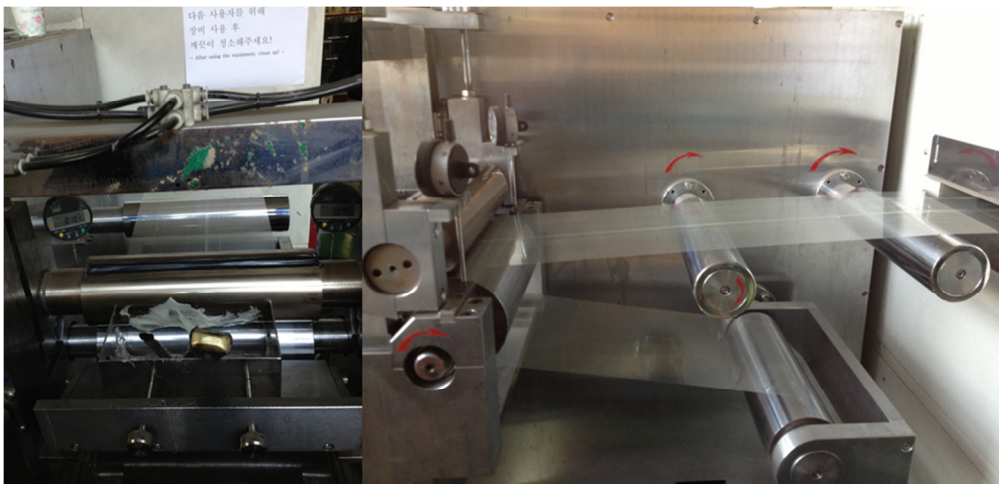

Figure 18. Images of film casting machine

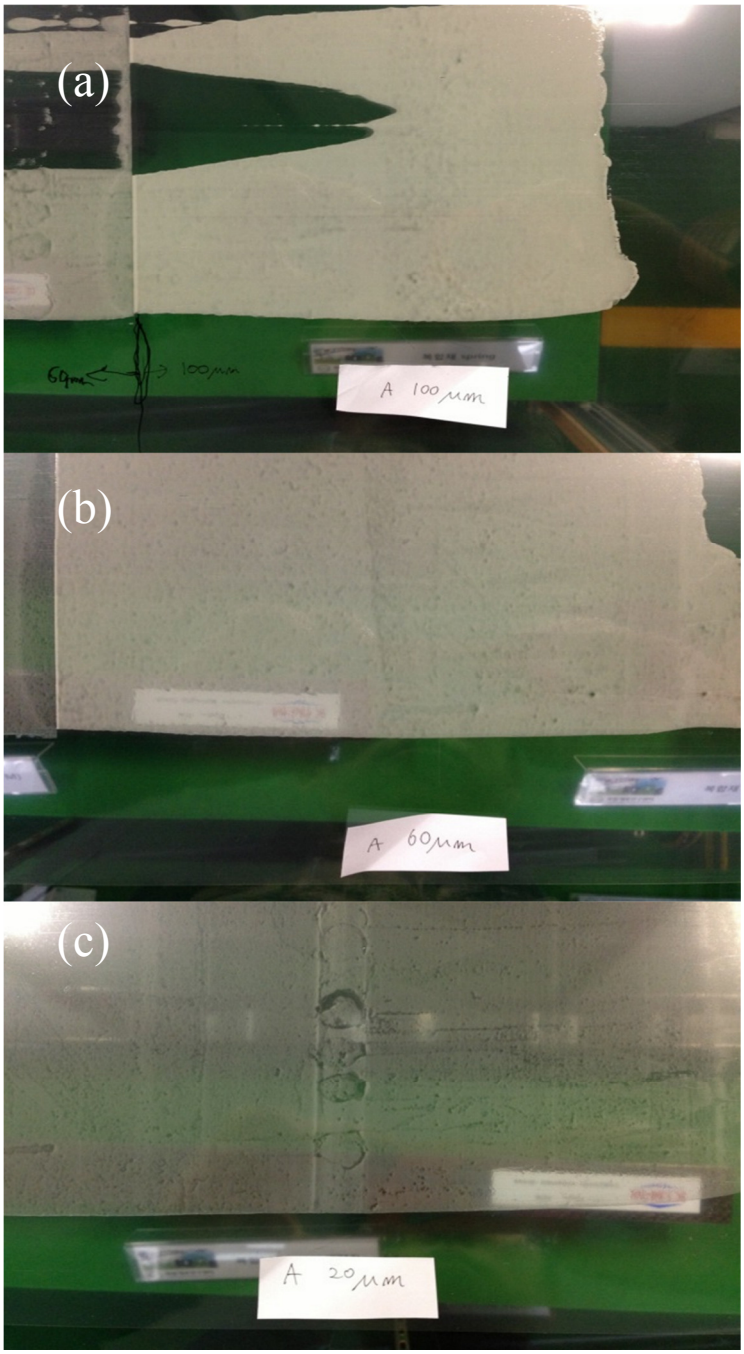

Figure 19. Images of resin film samples manufactured by each experimental conditions (a) thickness=100um, (b) thickness=60um, (c) thickness=20um

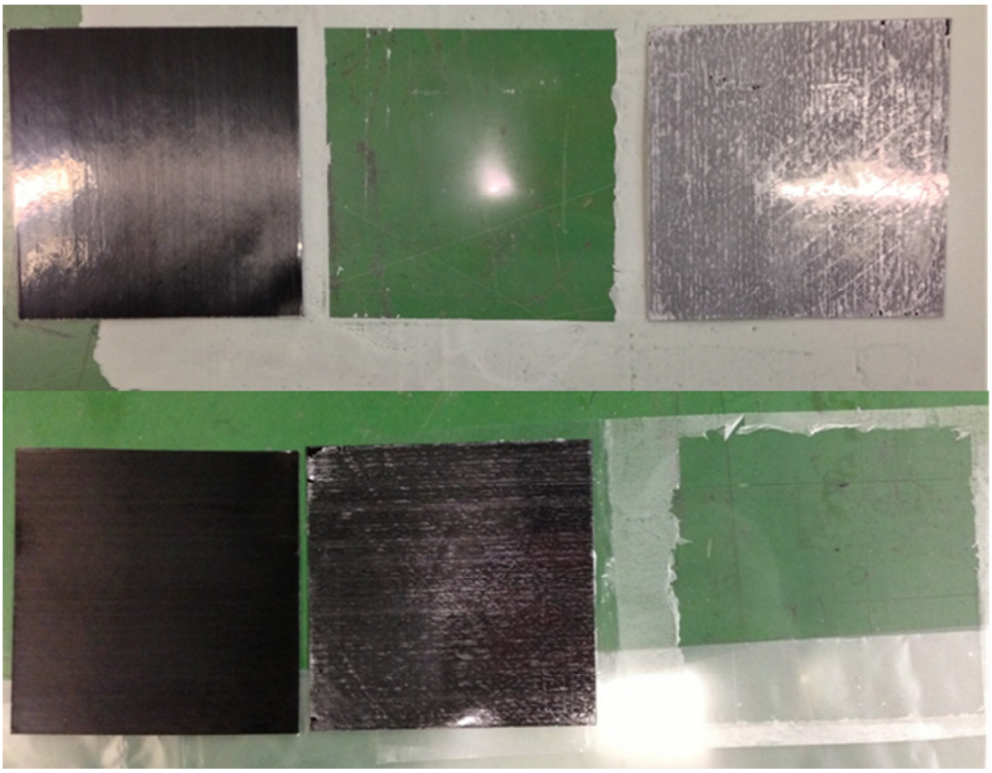

Figure 20. Image of perfectly transferred particles dispersed resin film to carbon fiber prepreg

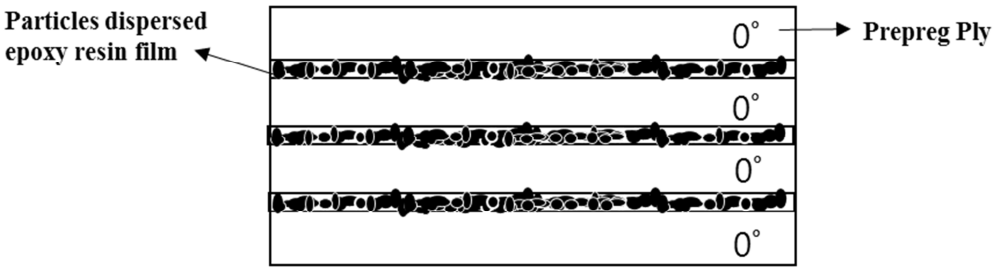

Figure 21. Scheme of carbon fiber reinforced plastic specimen with particles dispersed resin film

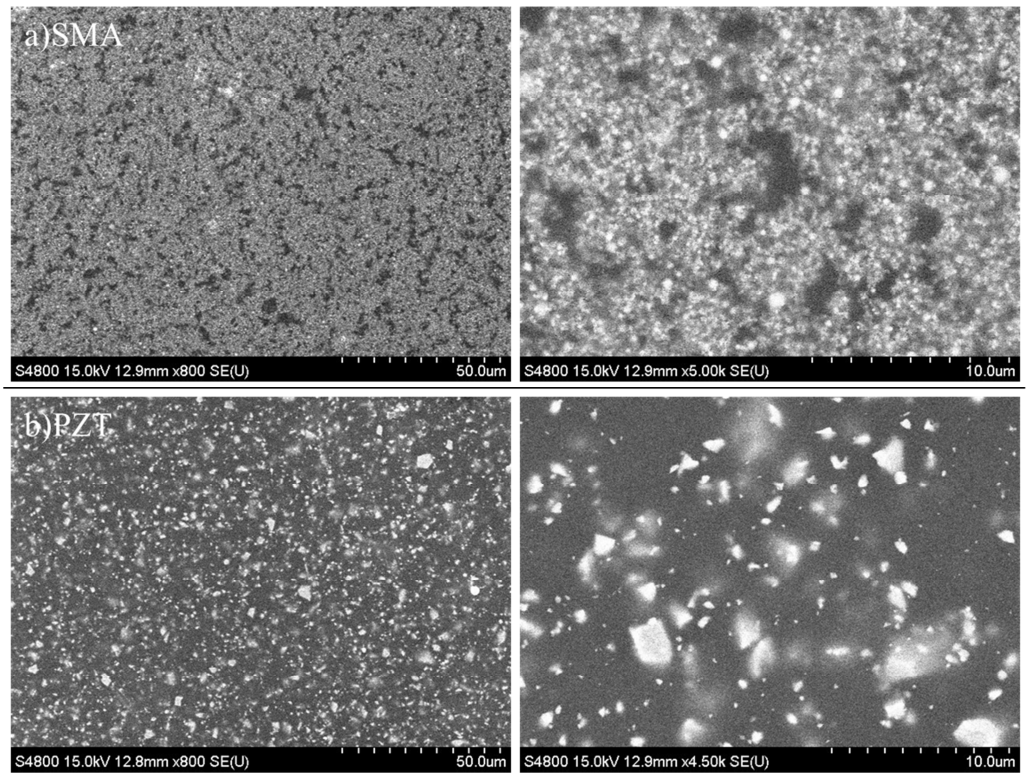

Figure 22. SEM image of (a) SMA and (b) PZT particles dispersed resin film

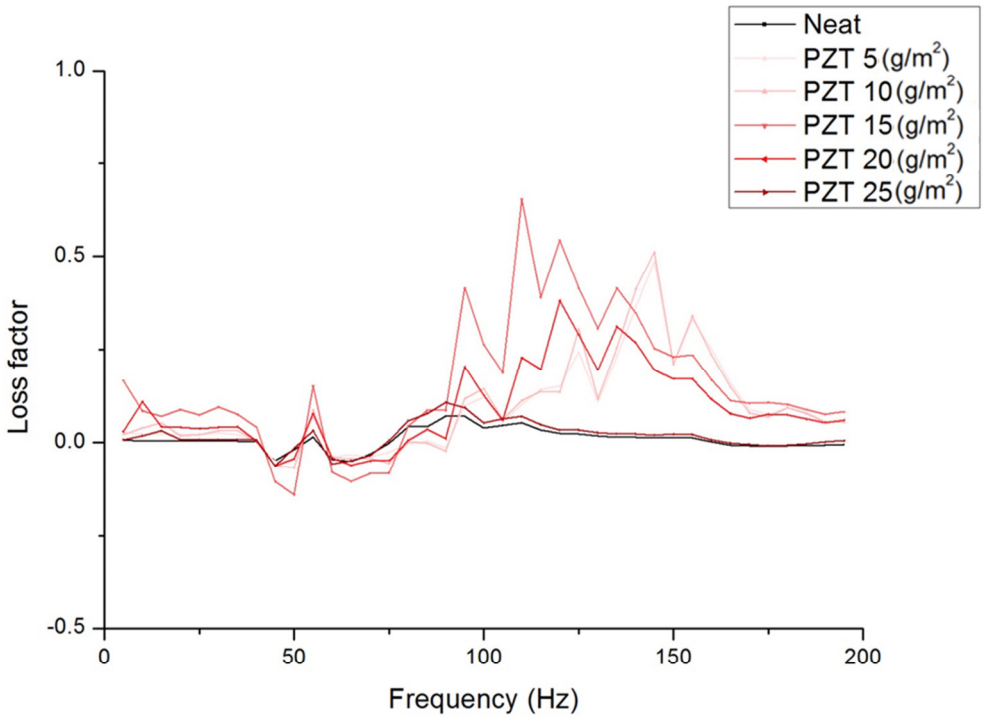

Figure 23. The loss factor of CFRP /PZT particles dispersed resin film along with frequency sweep

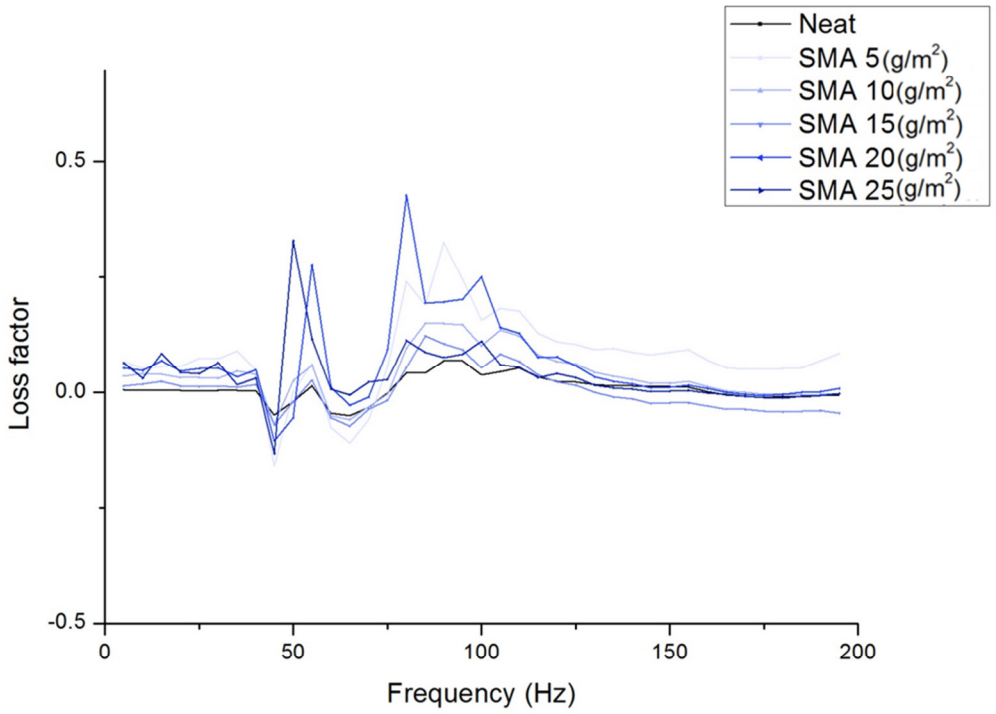

Figure 24. The loss factor of CFRP /SMA particles dispersed resin film along with frequency sweep

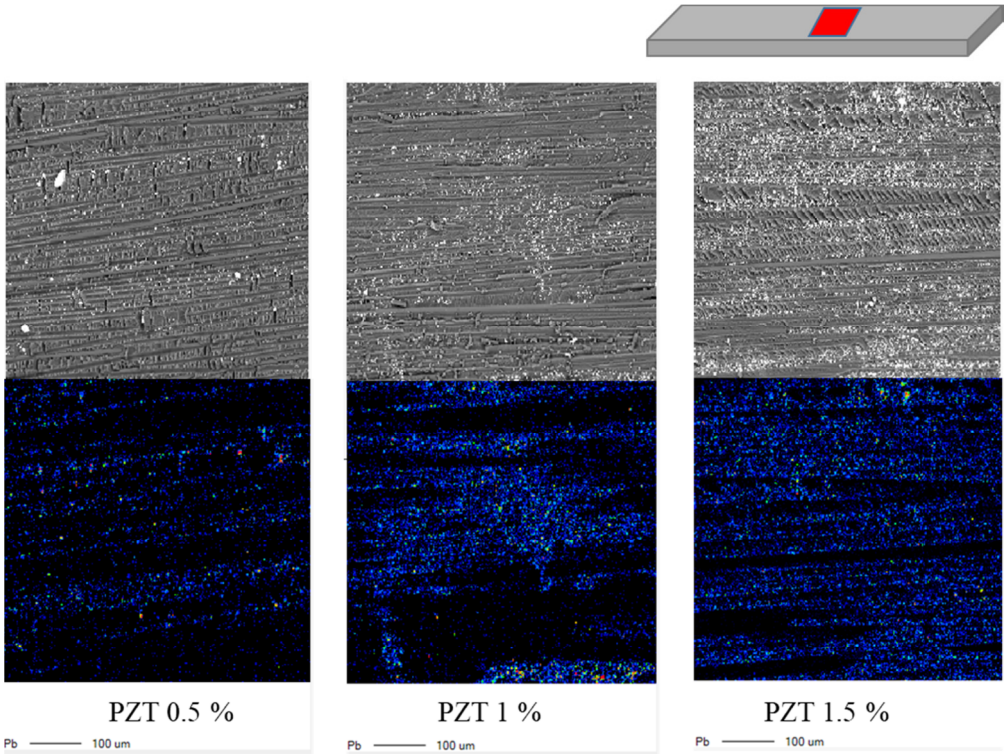

Figure 25. Evaluation of dispersion by mapping Pb (lead) element using EPMA (Electron probe micro analysis)

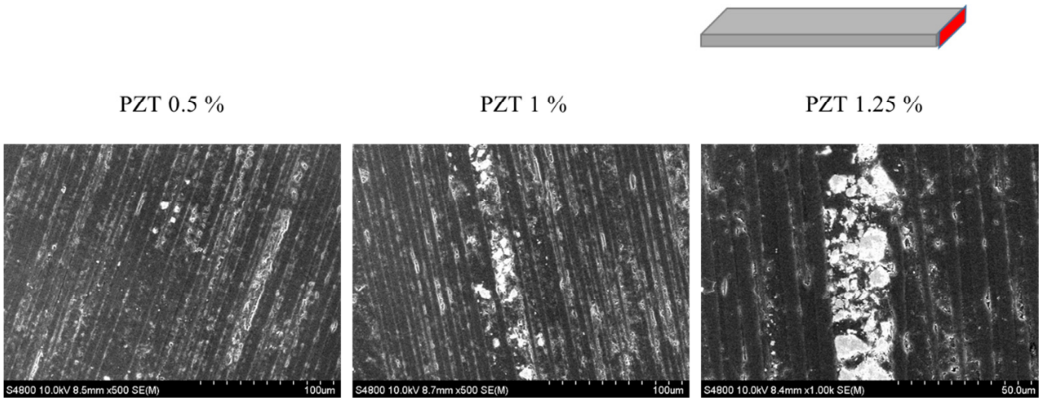

Figure 26. The fracture surface of the specimen was measured using SEM (Scanning electron microscope)

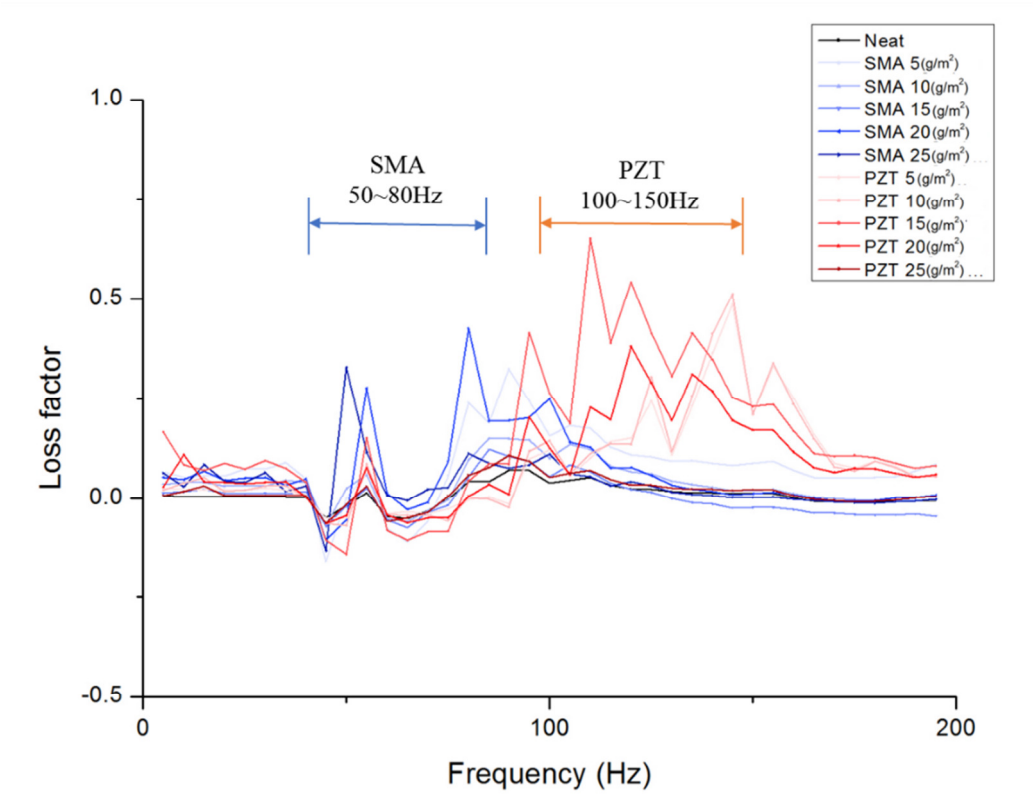

Figure 27. The loss factor of CFRP /PZT particles dispersed resin film and CFRP /SMA particles dispersed resin film

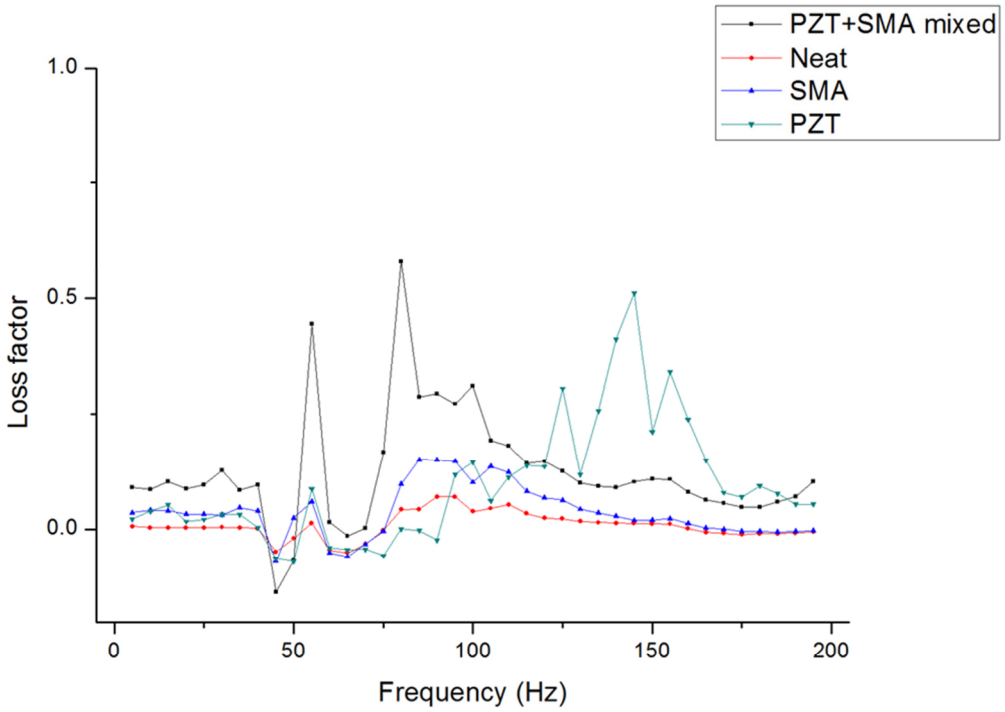

Figure 28. The loss factor of CFRP with PZT and SMA mixed particles dispersed resin film and comparison of the loss factor of CFRP with PZT alone and CFRP with SMA alone dispersed resin film

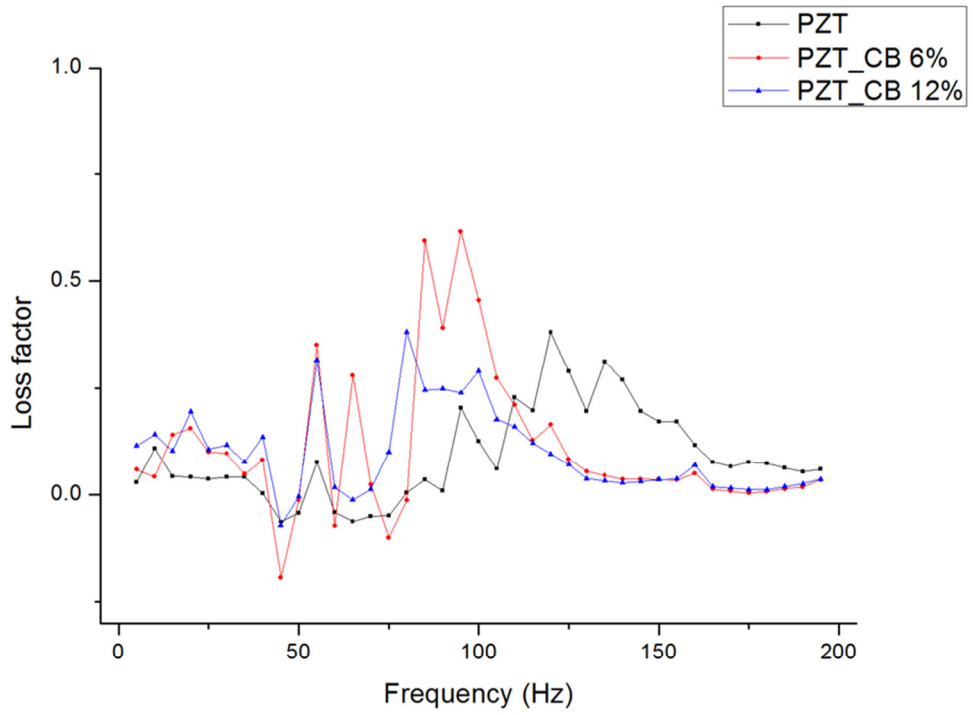

Figure 29. The loss factor of CFRP with PZT/ six weight percent carbon black particles dispersed resin film and comparison of the loss factor of CFRP with PZT alone and CFRP with PZT/ 12 weight percent carbon black particles dispersed resin film

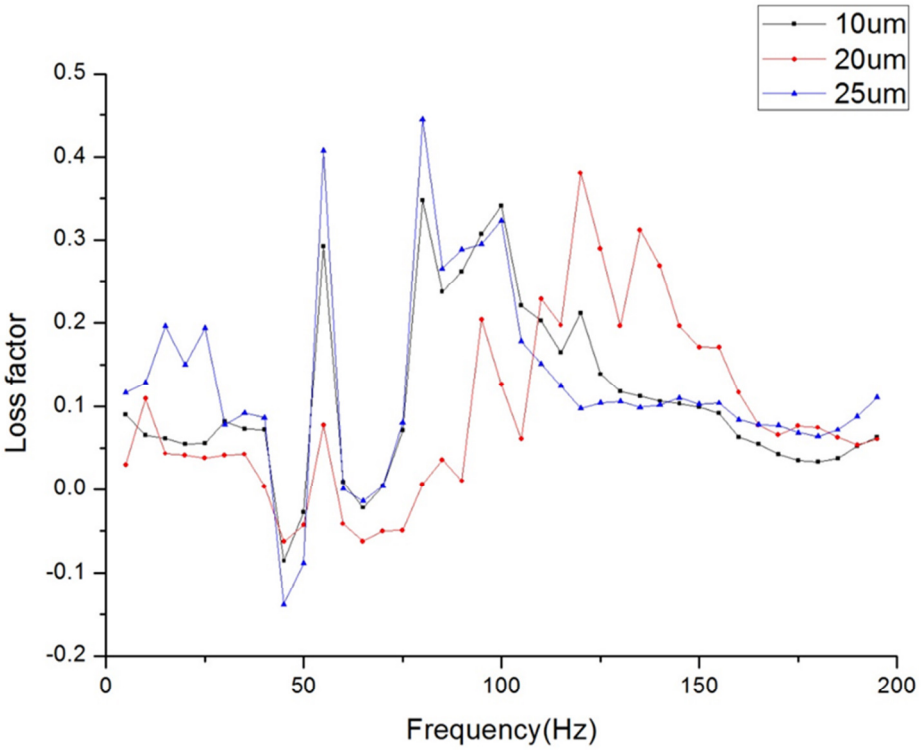

Figure 30. Comparison of the loss factor PZT particles with different size

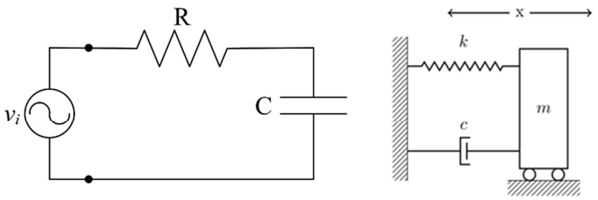

Resistance = Carbon fiber or conductive matrix

AC voltage = Piezoelectricity induced by U_m

Capacitance = capacitance of PZT

Figure 31. The concept of RC circuit and shunted piezoelectric circuit similarity

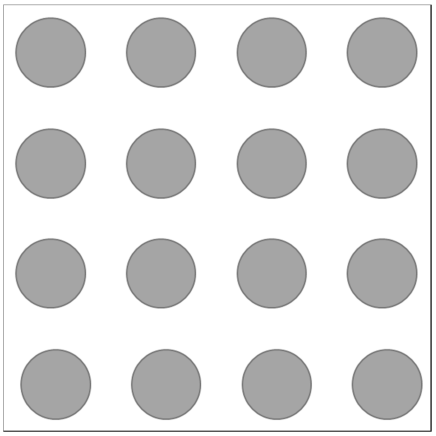

Figure 32. Simple cubic (SC) model

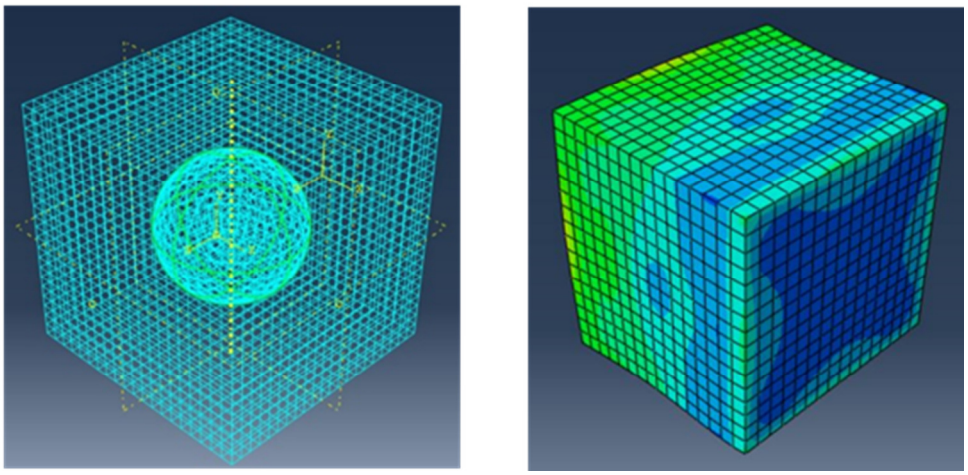

Figure 33. RVE model of 0-3 composite with spherical PZT particles

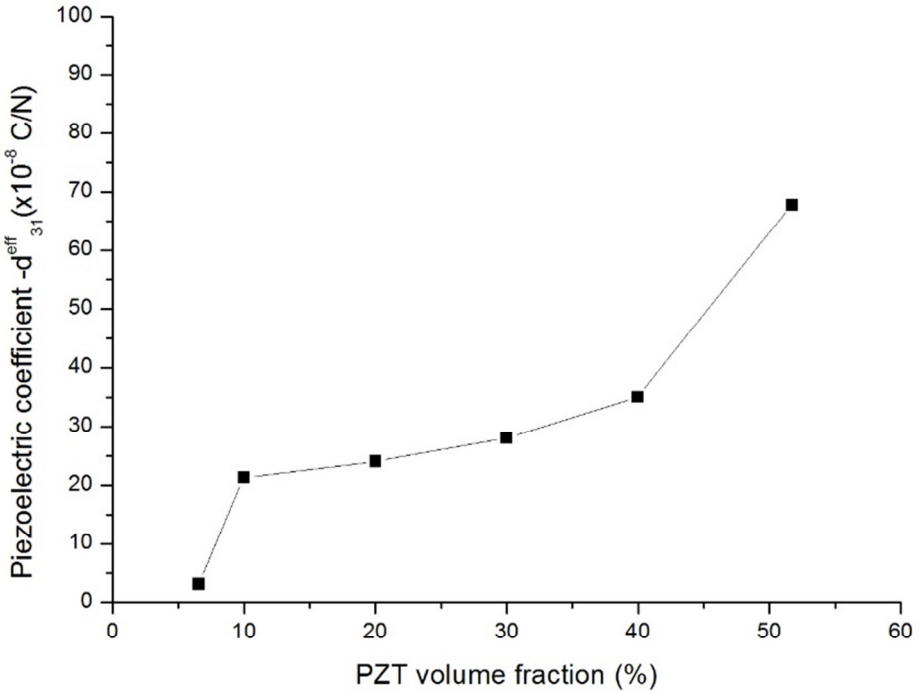

Figure 34. The relation between effective piezoelectric coefficient and the particle volume fraction

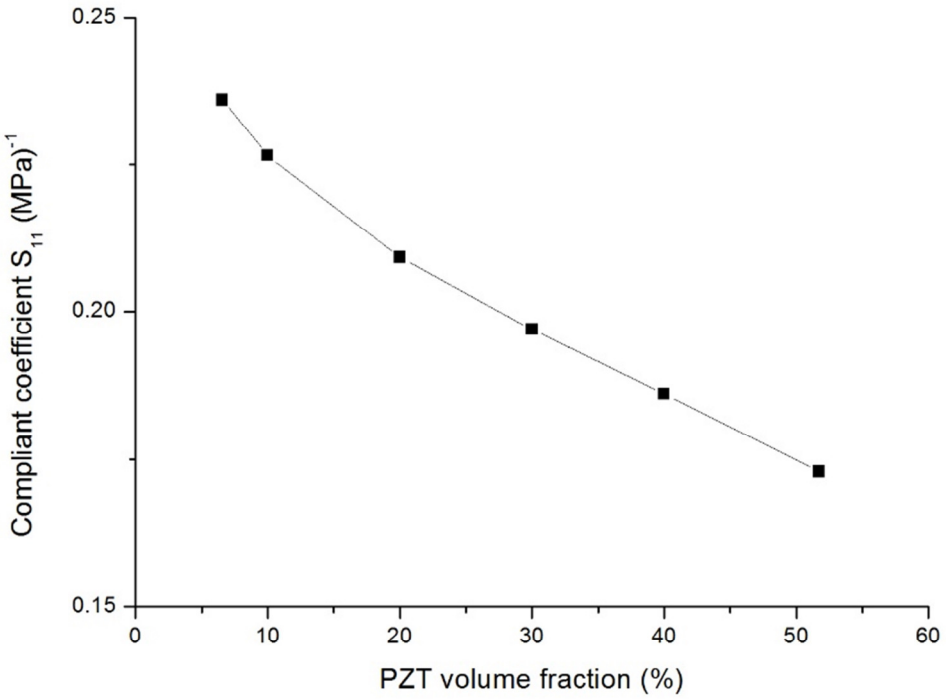

Figure 35. The relation between effective compliant coefficient and the particle volume fraction

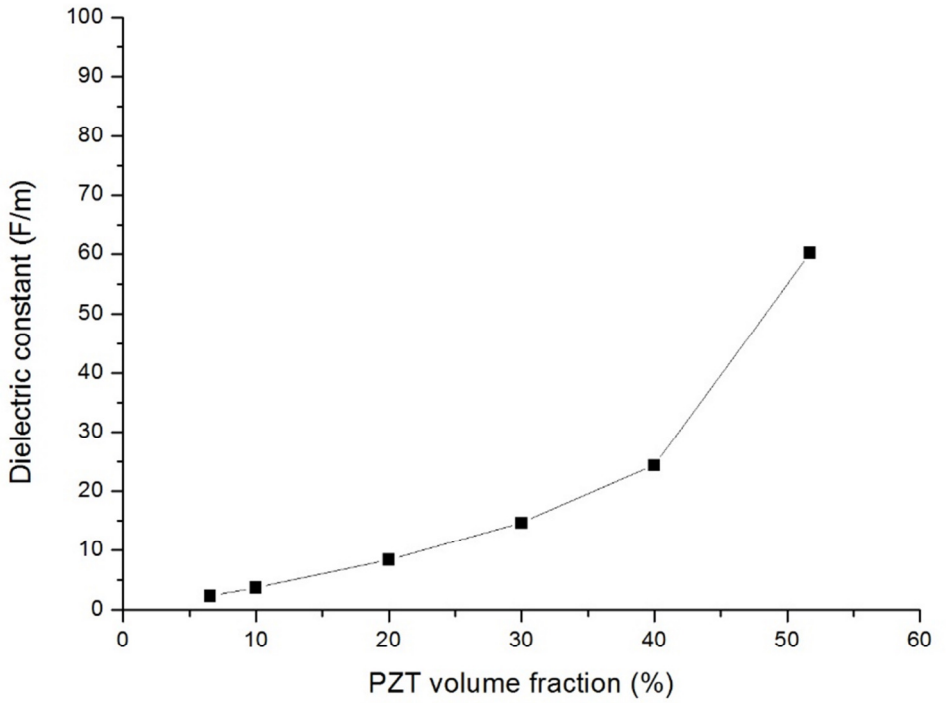

Figure 36. The relation between effective dielectric constant and the particle volume fraction

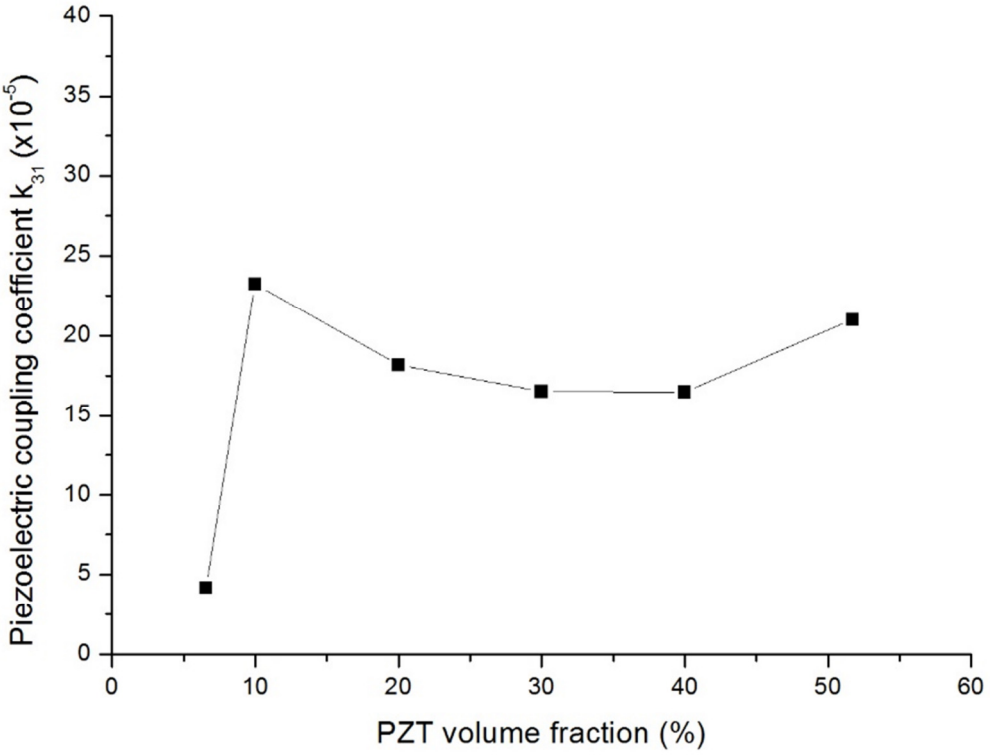

Figure 37. The relation between effective piezoelectric coupling coefficient and the particle volume fraction

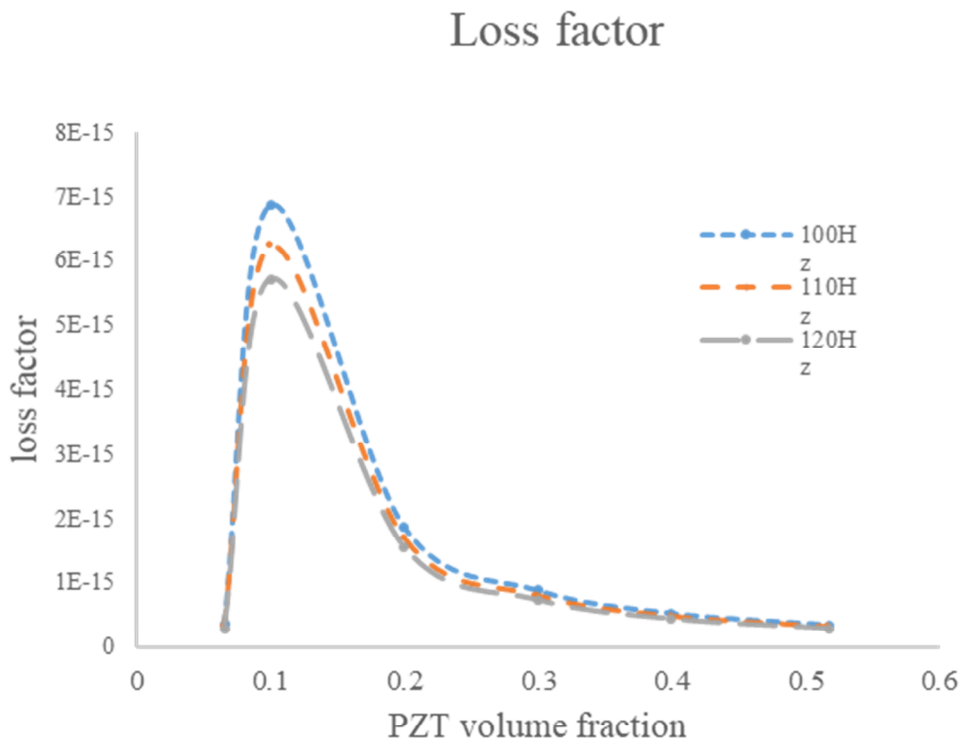

Figure 38. The relation between the loss factor and the particle volume fraction

Tables

Film Thickness	PZT loading
100um	$5g/m^2$
60um	
20um	

Table 1. PZT particles dispersed resin film manufacturing test conditions

	0g/m^2	5g/m^2	10g/m^2	15g/m^2	20g/m^2	25g/m^2
PZT	Resin only	1 types of particle size	1 types of particle size	1 types of particle size	3 types of particle size, CB 6wt%,12 wt%	1 types of particle size
SMA	Resin only	1 types of particle size	1 types of particle size	1 types of particle size	1 types of particle size	1 types of particle size

Table 2. The experimental conditions of various particles loading and types

	C_{11} (Gpa)	Poisson's Ratio	Density	ε_1^T	ε_3^T	d_{31} (pC/N)	d_{33} (pC/N)
Matrix	10	0.3	1.15	3.6	3.6	0	0
PZT	100	0.3	7.8	1980	2400	-280	500

Table 3. Properties of Matrix and PZT Particles

압전재료 입자와 형상기억합금 입자를 사용한 탄소섬유 강화복합재료의 진동감쇠향상

서울대학교 대학원
기계항공공학부
정 재 민

요약(국문초록)

탄소 섬유 강화 복합재료는 항공 우주, 자동차, 토목 공학 및 레저 및 스포츠 용품 산업과 같은 다양한 산업 분야에서 높은 강도 대비 가벼운 무게, 저밀도, 우수한 열 적 특성 및 기타 우수한 기계적 특성 때문에 널리 사용되어왔다. 그러나 이러한 장점에도 불구하고 낮은 진동 감쇠 능력으로 인해 많은 진동을 견뎌야 하는 일부 구조물에는 적용하는데 어려움이 따른다. 따라서 최근 CFRP 복합 재료의 진동 감쇠 향상에 대한 연구가 진행되고있다.

압전 세라믹 입자는 기계적 변형이 가해지면 전기적 에너지가 발생하는 압전 효과를 가지는 재료로, 본 연구에서 진동 에너지의 손실을 가속화시키는 기능성 입자로 사용되었다. 형상 기억 합금은 일반적으로 진동 감쇠 성능을 향상시킬 수 있는 일종의 초 탄성 물질로 알려져 있다. 재료의 형상이 바뀌면 그 위상과 결정 구조가 바뀌므로 기계적 에너지가 결과적으로 열에너지로 변환된다.

본 연구에서 탄소 섬유 강화 복합재료 내부에 압전 세라믹 입자 및 형상

기억합금 입자를 분산 시켜 높은 진동 감쇠 성능을 갖는 복합재료 제작 방안을 제안하였다. 진동 감쇠를 나타내는 지표인 손실 계수의 변화를 확인하기 위해 동역학적 기계 분석기를 사용하여 분석을 수행하였다.

본 연구를 통하여 압전 세라믹 입자와 형상기억합금 입자를 함유 한 탄소섬유강화복합재료의 진동 감쇠가 기존의 재료보다 높다는 것을 확인하였다. 또한 복합재료 내부에서 입자의 분산도가 진동 감쇠 능력을 결정하는 중요한 요소임을 확인하였다. 따라서 탄소섬유 강화 복합재료 내부에서 입자의 분산을 향상시키기 위해 입자가 분산 된 얇은 수지 필름을 제조하여 사용하였다. 이것을 복합재료에 적용함으로써, 분산도의 증가가 진동 감쇠 개선에 긍정적 인 영향을 미치는 것을 확인하였다. 마지막으로 실험 결과를 확인하고 매개 변수를 최적화하기 위해 다양한 매개 변수에 대한 수치 해석 연구를 병행하여 수행하였다.

주요어 : 진동 감쇠, 탄소섬유강화복합재료, 압전 효과, 형상기억합금, 손실계수, 동역학적 기계 분석기

학번 : 2011 – 20751